AN ABSTRACT OF THE THESIS OF

Sebastian Geiger for the degree of Master of Science in Geology presented on March 14, 2000. Title: Reactive Transport Modeling in a Discrete Fracture: Applications to the Formation of Sericitic Hydrothermal Alteration at Butte, Montana.

Abstract approved: Redacted for privacy

Roy Haggerty

A model for the spatial and temporal evolution of the gray sericitic (GS) and sericite with remnant biotite (SBr) hydrothermal alteration selvages within the Butte Quartz Monzonite (BQM) of the porphyry copper deposit at Butte, Montana, is presented. The model provides a mathematical description for the location and advance of multiple mineral reaction fronts during diffusive solute transport under quasi-stationary state conditions. A method for scaling initial mineral masses was developed to efficiently model the system for sufficient geologic time. Simulations show that a reducing, highly acidic, and low salinity fluid can produce the GS and SBr alteration selvages up to 5 cm wide during the time span of approximately one hundred years or less. Hydrothermal alteration causes little change in the porosity and pore diffusivity of the BQM. Mineral precipitation and dissolution act as sources and sinks for the solutes and impose additional concentration gradients on the solution, which changes solute transport. The hydrothermal alteration zones are characterized by a sequence of reaction fronts. The biotite dissolution front occurs closest to the fracture and marks the transition between the GS and SBr zone. The plagioclase dissolution front occurs farthest into the matrix and marks the edge of

unaltered BQM. From the mathematical description for multiple alteration fronts, it follows that once the sequence of reaction fronts is fully established, it must remain constant and the widths of reaction zones expand proportional to the square root of time. The relative widths of reaction zones into the wall-rock remain approximately constant to each other through time. The widths of reaction zones decrease along the fracture, because the rate of diffusion of reactive solutes in the rock matrix is lower than the rate of advection of the reactive solutes in the fracture.

Reactive Transport Modeling in a Discrete Fracture: Applications to the Formation of Sericitic Hydrothermal Alteration at Butte, Montana.

by

Sebastian Geiger

A THESIS

submitted to

Oregon State University

in partial fulfillment of
the requirements for the
degree of

Master of Science

Presented March 14, 2000
Commencement June 2000

Master of Science thesis of Sebastian Geiger presented on March 14, 2000

APPROVED:

Redacted for privacy

Major Professor, representing Geology

Redacted for privacy

Chair of Department of Geosciences

Redacted for privacy

Dean of Graduate School

I understand that my thesis will become part of the permanent collection of Oregon State University libraries. My signature below authorizes release of my thesis to any reader upon request.

Redacted for privacy

Sebastian Geiger, Author

ACKNOWLEDGEMENTS

I have met many great people during the course of this MS thesis who have greatly contributed to make this little research project a success. Most and foremost, I am thankful to my committee members Roy Haggerty, John Dilles, Mark Reed, and Robert Duncan. Roy, John, and Mark are not only great geologists who came up with this very exciting research project. They are also excellent teachers who laid my background for this work and had the ability to explain even the most complex processes in a way that made it seem simple and easy to understand. Furthermore, their enthusiasm during the course of this work was more than stimulating and they always had the time to discuss any of the frequent problems that I ran into. I am also thankful to Robert for taking the time and helping out as the graduate council representative on my committee. The contributions by the other members of the Oregon Butte Research Group, namely Cy Field, Bob Houston, Lihua Zhang, and Brian "The Pyrite Pirate" Rusk made a lot of this work possible.

This thesis would still be far away from completion without the relentless help of Stephan Matthäi of the Fluid and Ore Deposit Group at the Swiss Federal Polytechnic Institute at Zurich, so an incredibly great deal of thanks is directed to him. Stephan provided not only the code for the simulations, but also spent countless hours in getting me started with it and clearing the roadblocks that came across more than once. A thanks also goes to two other people of the Fluid and Ore Deposit Group who have helped with some very useful comments: Chris Heinrich

and Thomas Driesner. Furthermore, I am greatly indebted to Carl Steefel of the Lawrence Livermore National Laboratory for many helpful discussions and suggestions and his overall interest in this work. Two people, who were influential during my earlier education, should not be forgotten here: my old high-school chemistry teacher Elin Ganter and Meinert Rahn of the University of Freiburg.

I would never have been able to pursue my degree at Oregon State without the help and financial support of the Radiation Center at Oregon State, where I was offered a research assistantship. Special thanks therefore go to Erwin Schütfort, Steve Binney, and Brian Dodd at the Radiation Center.

Numerous friends were always available to provide some welcome relief from my work and have made my time here unforgettable. Because of them I will take so much more than just a degree back to Europe. In no specific order, I am especially thankful to Derik Kleibacker, Nicolai Thum, Claudius von Schwerin, Carrie Mock, Jennifer Simeon, Francois Baratange, Renellys Perez, Bertrand Dano, Brandy Kuebel, Dan Diehl, Wendy Mitteager, Christine Lomas, Marilyn Lawson, Stacy Kish, Heiko Thoemen, Tim Driscol, Joel Pritchard, and Jennifer Myers. My old friends from Europe, Achim Poppensieker (especially him!), Stephan Rehm, Lara Springer, and Jürgen Eisele should also be thankfully mentioned here for not forgetting about me, although I lived several thousand miles away from them.

Last but certainly not least, I would like to thank my parents Helma and Karl-Georg, and my brother Christian for all their guidance, support, and encouragement even over such a long distance.

CONTRIBUTION OF AUTHORS

Roy Haggerty, John H. Dilles, and Mark H. Reed were the principal investigators of the research project that resulted in the manuscripts presented here. Their contributions included the assistance with initial development of the research problem, guidance throughout the course of this work, and help with the interpretation of the simulated results.

Stephan K. Matthäi contributed significantly to this project by supplying the reactive transport code CSP3D3.0 (Matthäi and Roberts, 1999) used in the simulations, and helping with the model set up and any problems during the course of the simulations.

TABLE OF CONTENTS

TABLE OF CONTENTS CONTINUED

TABLE OF CONTENTS CONTINUED

LIST OF FIGURES

LIST OF TABLES

LIST OF APPENDIX FIGURES

Reactive Transport Modeling in a Discrete Fracture: Applications to the Formation of Sericitic Hydrothermal Alteration at Butte, Montana.

CHAPTER I

INTRODUCTION

Many processes in the earth's crust can be understood as a combination of the transport of heat and solutes by a fluid, and the chemical interaction between the solid phase and the fluid (c.f., Steefel and MacQuarrie, 1996; Wood, 1997). Such processes are commonly called "reactive transport". The interactions usually involve diffusion, advection, dispersion, sorption, heat transfer between the fluid and the geologic medium, and mineral dissolution and precipitation.

During reactive transport, the physical and chemical properties of both the fluid and the geologic medium are changed over time and space (c.f., Steefel and MacQuarrie, 1996). Mineral precipitation and dissolution can change the porosity and permeability of the geologic medium. This can result in an altered flow regime and modified solute transport behavior. Furthermore, dissolution and precipitation of minerals can act as sources and sinks for solutes. Since mineral concentrations are usually much larger than solute concentrations, fluid-rock interactions can impose new concentration gradients on the fluid and can therefore change solute transport, fluid composition, and fluid density (c.f., Lichtner, 1996). In turn, the modifications in flow regime, solute transport, and fluid composition can affect the

subsequent fluid-rock reactions. As such, reactive transport therefore may result in a strongly nonlinear system with significant positive and negative feedbacks.

Examples of reactive transport include hydrothermal alteration (e.g., Steefel and Lasaga, 1994), diagenesis (e.g., Wang and Van Capellen, 1996), weathering (e.g., Soler and Lasaga, 1998), and metamorphism (e.g., Lasaga and Rye, 1993). Reactive transport has also been applied to groundwater remediation (e.g., Brown et al., 1998), biodegradation, (e.g., Wood et al., 1995), and nuclear waste disposal (e.g., Viswanathan et al., 1998).

Alteration envelopes in hydrothermal systems that form along fractures are excellent examples of reactive transport in the geologic environment. In hydrothermal alteration envelopes, solutes of a hydrothermal fluid diffuse between the fracture or vein channel and the surrounding rock where they chemically react with the wall-rock to alter its chemical composition and mineralogy (c.f., Reed, 1997). Chemical reactions that occur during high temperature and pressure over long time spans are preserved in the hydrothermal alteration envelopes. Since it is very difficult to study the development of alteration envelopes experimentally, reactive transport simulations offer an excellent tool to understand the spatial and temporal evolution of hydrothermal alteration zones. However, the evolution of hydrothermal alteration envelopes has rarely been studied quantitatively using reactive transport simulations because of the mathematically complex nature of the system, uncertainties in the physical and chemical parameters, sparse field data, and the large amount of computing time required to simulate adequate geologic time.

In this study, the spatial and temporal evolution of the early hydrothermal alteration systems of the porphyry copper deposits at Butte, Montana, is studied using reactive transport simulations. The object-oriented finite element C++ code CSP3D3.0 (Matthäi and Roberts, 1999) is applied for the simulations. CSP3D3.0 allows to simultaneously model fluid flow, solute transport, fluid-rock interactions, and deformation in a geologic medium.

Butte is a good example to study fossil hydrothermal alteration envelopes, because the petrology of the alteration zones at Butte is well-studied (e.g., Sales and Meyer, 1948; Meyer et al., 1968; Brimhall, 1977; Reed, 1979; Brimhall, 1980; Brimhall and Ghiorso, 1983). Furthermore, the most prominent alteration type of the early hydrothermal alteration at Butte (i.e., the sericitic pre-Main Stage alteration) occurs also in many other porphyry copper deposits around the world (Lowell and Guilbert, 1970; Gustafson and Hunt, 1975; Dilles and Einaudi, 1992). Understanding the evolution of the sericitic pre-Main Stage alteration at Butte therefore offers insight about the evolution of a prevalent alteration type.

The coupling of the physics of solute transport in a fracture with the chemistry of water-rock interactions at Butte leads to a series of key questions that are addressed in this study:

1. How can the spatial and temporal development of the mineral reaction fronts be described mathematically?
2. How do mineral reaction fronts in high-temperature and pressure systems develop spatially and temporally?
3. What is the feedback between reaction and solute transport, i.e., how does hydrothermal alteration affect solute transport?
4. What is the composition of the hydrothermal fluid that generated the known mineral assemblages at Butte?
5. What is the time frame for the alteration envelopes observed at Butte?

Using vein geology, geochemical modeling, and intensive forward modeling of reactive transport in a discrete fracture with an infinite matrix, the evolution of the observed early hydrothermal alteration systems at Butte is simulated to address the questions outlined.

The results of the reactive transport simulations presented this thesis are divided into two chapters, both of which will be submitted for publication in peer-reviewed journals. The first chapter, which is for a potential submission to the a peer-reviewed journal depending on some further results, focuses on the physics of reactive transport and gives a general quantitative description of the spatial and temporal development of multiple mineral reaction fronts. The paper discusses the quantitative treatment of reactive transport, i.e., how the spatial and temporal evolution of mineral reaction fronts can be described mathematically under the

assumptions that diffusion is the governing solute transport process and that water-rock reactions occur under transport-limited conditions. Most of the key properties of such a system were derived by Lichtner (1988), Novak et al. (1989), Lichtner (1991), Lichtner and Balashov (1993), and Steefel and Lichtner (1998) and follow from the quasi-stationary state approximation (Lichtner, 1988; 1991). The paper develops the scaling properties of reactive transport models, which are critically important for the simulation of geologic systems. In an example application of the principles, the results of numerical simulations for the early hydrothermal alteration at Butte are then discussed.

The second paper, which will be submitted to *Economic Geology*, focuses on the application of reactive transport modeling to the gray sericitic pre-Main Stage alteration at Butte. The gray sericitic alteration at Butte is similar to sericitic (phyllic) alteration that is common at many other porphyry copper deposits around the world (c.f., Lowell and Guilbert, 1970; Gustafson and Hunt, 1975; Dilles and Einaudi, 1992). The paper therefore explains the spatial and temporal evolution of a prevalent hydrothermal alteration process. The feedback between hydrothermal alteration and water-rock reactions is also assessed and a possible composition of the hydrothermal fluid that could have formed the observed alteration zones has been derived.

CHAPTER II

ON THE EVOLUTION OF HYDROTHERMAL ALTERATION FRONTS: MULTI-COMPONENT DIFFUSION AND REACTION, QUASI-STATIONARY STATE CONDITIONS, AND MASS-SCALING PROPERTIES

Sebastian Geiger [†], **Roy Haggerty, John H. Dilles**

Department of Geosciences, Oregon State University, Wilkinson Hall,

Corvallis, OR 97331-5506, U.S.A

Mark H. Reed

Department of Geological Sciences, 1272 University of Oregon,

Eugene, OR 97403-1272, U.S.A

Stephan K. Matthäi

Department of Earth Sciences, Swiss Federal Institute of Technology (ETH),

NO Building, Sonneggstr. 32, CH-8092 Zurich, Switzerland

[†] Corresponding author: e-mail, Sebastian.Geiger@orst.edu

For possible submission

A_Ω	Flux area [L^2]
C_n	Concentration of aqueous species [M L^{-3}]
C_{eq}	Concentration in equilibrium with mineral [M L^{-3}]
C_o	Concentration at inlet of porous column [M L^{-3}]
D_p	Pore diffusivity [L^2 T]
F_m	Scaling factor for mineral mass [-]
F^*	Scaling factor for time or space [-]
J	Number of chemical elements [-]
M	Number of solids [-]
M_f	Mass fluid [M]
N	Number of aqueous species [-]
S_m	Mass of solid [M]
S_m^∞	Initial mass of solid [M]
V_f	Volume Fluid [L^3]
V_M	Molar mineral volume [L^{-3} M]
V_s	Volume Solid [L^3]
V_{tot}	Total volume solid and fluid [L^3]
t	Time [T]
u_f	Darcy velocity [L T^{-1}]
$v_m(t)$	Velocity of mineral reaction front [L T^{-1}]
x	Distance normal to the fracture [L]
$x_m(t)$	Location of mineral reaction front [L]
ΔC	Concentration gradient [M L^{-3}]
$\Delta x_m(t)$	Difference in location of a reaction front [L]
Ξ_m	Total elemental concentration of solid [M L^{-3}]
Ω_j	Generalized diffusive flux [M T^{-1} L^{-2}]
Ω_j^C	Generalized diffusive flux in terms of a change in concentration [M T^{-1} L^{-2}]
Ω_j^S	Generalized diffusive flux in terms of a change in solid mass [M T^{-1} L^{-2}]
β_k	Constant for velocity of mineral reaction front [-]
η	Similarity variable [-]
ν_{jm}	Stoichiometric reaction matrix of solid [-]
ν_{jn}	Stoichiometric reaction matrix of aqueous species [-]
ϕ	Porosity [-]
ϕ_m	Mineral volume fraction [-]
ϕ_R	Total reactive volume fraction [-]
ψ_j	Total elemental concentration of aqueous species [M L^{-3}]
ρ_m	Density solid [M L^{-3}]
ρ_f	Density fluid [M L^{-3}]
ρ_{mV}	Mineral bulk density [M L^{-3}]
$\sigma_m(t)$	Slope of alteration front [-]

Table II.1. List of Symbols

II.1 Abstract

The quasi-stationary state approximation (Lichtner, 1988; 1991) allows the quantitative description of the spatial and temporal evolution of mineral reaction fronts, such as occurring in the sericitic pre-Main Stage hydrothermal alteration at Butte, Montana. An analysis of the quasi-stationary state approximation shows that initial mineral masses in reactive transport simulations can be scaled, which provides an efficient way to simulate for adequate geologic time. Fluid-rock reactions in hydrothermal alteration selvages are transport-limited and solute transport is diffusion-controlled. Reaction fronts are characterized by narrow widths, which explains the sharp transition between fresh and altered rock. Since the location of multiple reaction fronts depends on the concentration gradient and solute flux across the reaction front, the relative location of the reaction fronts remains constant through time. Reaction zones grow with time but maintain a constant ratio of widths to each other. Reactive transport simulations carried out for the sericitic pre-Main Stage alteration at Butte, Montana, show the behavior predicted by the derived mathematical formulations.

II.2 Introduction

Hydrothermal alteration envelopes on veins, such as occurring in e.g., Butte, Montana (Meyer et al., 1968; Brimhall, 1977) are prime examples of reactive transport. Hydrothermal alteration envelopes evolved under high pressure

and temperature during long time spans. It is therefore difficult to study the evolution of alteration envelopes experimentally, but reactive transport simulations can yield insights about the development of the alteration zones (e.g., Geiger, 2000). The development of these alteration envelopes is governed by multi-component diffusion and reaction. Intrinsic reaction rates are commonly fast, so that the local equilibrium assumption can be applied (c.f., Reed, 1997).

The quasi-stationary state approximation (Lichtner, 1988; 1991) is commonly used to describe the evolution of mineral reaction zones. A key point of the quasi-stationary state approximation is that the mineral concentration (i.e., the mass of a mineral per unit volume of fluid) is much larger than the solute concentration and that consequently the movement of any reaction front is much slower than the rate at which diffusion comes to steady state (Lichtner, 1988; 1991). Therefore, for a particular mineral assemblage, solute concentrations are fixed. Changes in concentration happen only as the result of the advance of the alteration envelope, and are therefore considered "quasi-stationary" (Lichtner, 1988; 1991). The term "quasi-stationary" therefore means approximately the same as the term "rock-buffered" used in hydrothermal geochemistry.

Lichtner (1988; 1991) derived many of the relationships that yield important understanding of the spatial and temporal development of reaction fronts during multi-component diffusion and reaction. For example, if diffusion is the governing transport process, then the location of a reaction front changes as the square root of time (Lichtner, 1988; 1991). The thickness of reaction zones

therefore increases with the square root of time and hence the ratio of the widths of two reaction zones must remain constant (Lichtner, 1988; 1991).

Furthermore, Novak et al. (1989) showed that the governing equation for diffusive transport and reaction is self-similar, meaning that the solution for any one time is obtained simply by scaling the solution from any other time. Lichtner and Balashov (1993) have also shown that so-called "ghost zones" can form in the limit of pure advection. Ghost zones are mineral reaction zones that maintain a constant width as the zone advances through the rock (Lichtner and Balashov, 1993). In a recent study, Steefel and Lichtner (1998) have derived a formulation for the geometries of alteration fronts during reactive solute transport in a discrete fracture with matrix diffusion. This formulation gives an explanation for phenomena commonly observed in hydrothermal alteration zones. These phenomena include wedging of the alteration halos and the pinching out of alteration envelopes along discrete fractures.

One of the problems related to multi-component diffusion and reaction modeling of hydrothermal systems is the efficient coupling of the transport and reaction steps. Fully decoupled models that make use of methods such as the sequential iterative approach (SIA) (Yeh and Tripathi, 1989; Yeh and Tripathi, 1991; Zysset et al., 1994), the sequential non-iterative approach (SNIA) (Valocchi and Malmstead, 1992), or the strang splitting method (Zysset and Stauffer, 1992) often require large computing time to simulate for geologic time. In systems involving a complex series of chemical reactions, calculating the reaction step can

significantly slow down the simulations (Geiger, 2000). The accuracy of the results is also strongly dependent on the size of the time-step in decoupled models, and small time-stepping is often required to obtain reasonable results.

In this paper we will first discuss the basic equations that describe the evolution of mineral reaction fronts in a pure diffusive system, specifically under quasi-stationary state conditions. We will then derive mass-scaling properties from those equations and apply mass scaling to a simple reactive transport model where microcline is altered to muscovite. Finally, we will show the implications of the equations and mass scaling by applying them to the fossil hydrothermal alteration at Butte, Montana, and explain how the evolution of the alteration assemblages can be predicted.

II.3 Mathematical Formulation for Multi-Component Diffusion and Reaction

The mass balance equation for multicomponent diffusion and reaction in one dimension for a system containing M minerals of mass S_m, N aqueous species of concentration C_n, and a total of J chemical components, can be written as (Novak et al., 1989; Lichtner and Balashov, 1993)

$$\frac{\partial}{\partial t}\left(\phi\psi_j\right)=\frac{\partial}{\partial x}\left(\phi D_p\frac{\partial\psi_j}{\partial x}\right)+\frac{\partial\Xi_j}{\partial t} \qquad (1)$$

where D_p is the pore diffusivity and ϕ is the porosity. The elemental totals of the aqueous species ψ_j are given by the sum of the concentrations, C_n, of all aqueous species and the aqueous stoichiometric matrix ν_{jn}

$$\psi_j = \sum_{n=1}^{N} \nu_{jn} C_n \qquad j = 1,.....J \tag{2}$$

The elemental totals of the solid phases Ξ_m are given by the sum of the mineral masses, S_m, of all minerals and the solid stoichiometric matrix ν_{jm}

$$\Xi_j = \sum_{m=1}^{M} \nu_{jm} S_m \qquad j = 1,.....J \tag{3}$$

Fulfilling the quasi-stationary state approximation $\partial\psi_j/\partial t \approx 0$ (Lichtner, 1988), equation (1) reduces to

$$\frac{\partial \Xi_j}{\partial t} = -\frac{\partial}{\partial x}\left(\phi D_p \frac{\partial \psi_j}{\partial x} \right) \tag{4}$$

The appropriate boundary conditions for equation (4) are given by the Rankine-Hugoniot Equations (Lichtner, 1985; 1988; 1991)

$$[\psi_m]_{x_m(t)} = \psi_j^{(-)}(x_m(t)) - \psi_j^{(+)}(x_m(t)) = 0 \tag{5}$$

and

$$[\Omega_j]_{x_m(t)} = \Omega_j^{(-)}(x_m(t)) - \Omega_j^{(+)}(x_m(t)) = 0 \tag{6}$$

where $x_m(t)$ is the location of the mineral reaction front. The j^{th} generalized diffusive flux of the total element concentration ψ_j of species j is referred to as Ω_j. The change in total element concentration ψ_j and in the generalized diffusive flux Ω_j across the reaction front $x_m(t)$ is denoted by the square brackets $[\ldots]x_m(t)$, where

the superscript (+) depicts concentration to the right and (-) to the left hand side of the reaction front. In a purely diffusive system, Ω_j is given as the concentration gradient $\Omega_j = -\phi D_p(d\psi_j/dx)$. If chemical reactions are infinitely fast, it is therefore only necessary to solve the set of partial differential equations given in (4) (Lichtner, 1988).

Novak et al. (1989) showed that for constant boundary conditions and porosity, equation (1) can be transformed from a partial differential equation to an ordinary differential equation by introducing the similarity variable η. The transformation into η -space gives a definitive solution for pure diffusive multi-component transport and reaction (Novak et al., 1989). The mass balance equation at quasi-stationary state (Equation 4) can be similarly transformed (Lichtner and Balashov, 1993). The similarity variable η is defined as

$$\eta = \frac{x}{2\sqrt{D_p t \phi}} \tag{7}$$

which gives the ordinary differential equation

$$\frac{d^2\psi_j}{d\eta^2} - 2\eta\frac{d\Xi_j}{d\eta} = 0 \tag{8}$$

Equation (8) represents a tremendous simplification to the transient mass balance equation for multi-component diffusion and reaction (Equation 1). It can be shown from (8) that in η-space the location of a mineral reaction front $x_m(t)$ is fixed (Lichtner, 1991; Lichtner and Balashov, 1993)

$$x_m = 2\beta_k\sqrt{D_p t} \tag{9}$$

where β_k is a constant, which is different for every mineral reaction front, and is given by

$$\beta_k = \frac{\phi}{2} \frac{\left[\frac{d\psi_j}{d\eta}\right]_{x(t)_m}}{\sum_m \nu_{jm} V_M^{-1} \left[\phi_m\right]_{x(t)_m}} \tag{10}$$

The molar volume of a mineral is V_M; the mineral volume fraction is ϕ_m. The general expression for the velocity of a reaction front $v_m(t)$ in a diffusion controlled multi-component system similarly follows from the generalized Rankine-Hugoniot equation (Lichtner, 1985; 1988; 1991)

$$v_m(t) = \frac{\left[\Omega_j\right]_{x(t)_m}}{\sum_{m=1}^{N_{\min}} \nu_{jm} V_M^{-1} \left[\phi_m\right]_{x(t)_m}} \tag{11}$$

II.4 Mass Scaling

II.4.1 Mathematical Formulation

The similarity variable η equation (7) yields some important understanding for the evolution of mineral reaction zones. The similarity variable shows that the aqueous and mineral concentrations are identical for any combination of x, D_p, ϕ, and t that yield the same value of η. This means that reaction fronts have constant locations in η-space (Novak et al., 1989). Furthermore, the similarity variable requires that if one of the parameters x, D_p, ϕ, or t is scaled, a second parameter must be scaled accordingly to keep η constant.

The scaling analysis conducted by Lichtner (1993) raises the question of whether parameters other than the reaction rate coefficients can be scaled in equations (1) and (4) to increase the efficiency of reactive transport simulations. In this section, we will specifically focus on the scaling of parameters under quasi-stationary state conditions (i.e., equation (4)).

It appears that scaling the initial porosity in (4) and (7), respectively, via the initial mineral mass S_m^∞ is a good choice, because an aqueous solution composition is independent of the mass of saturated minerals (Reed, 1998). This means that the concentration of a solution is constant, no matter if the solution is e.g., in equilibrium with 10 or 100 moles of a specific mineral. However, if a hydrothermal fluid attacks an undersaturated mineral, it takes a longer time to dissolve the mineral if its mass is large. This suggests that if the initial mass of a mineral is scaled by some factor F_m less than one, the mineral dissolves faster in the simulation. In the results, time, t, or distance, x, must therefore be re-scaled by some factor F^* related to F_m in order to keep η constant.

The porosity ϕ is related to the mineral mass S_m via the sum of the mineral volume fractions $\Sigma\phi_m$ in the conservation of volumes (Lichtner, 1988)

$$\phi + \sum_{m=1}^{M} \phi_m = \phi_R = 1 \tag{12}$$

where the total reactive volume fraction is ϕ_R. If a single component system is assumed for simplicity and ϕ, $\Sigma\phi_m$, and ϕ_R in (12) are expressed in terms of fluid

mass, M_f, fluid density, ρ_f, initial mineral mass, S_m^{∞}, mineral density, ρ_m, and total volume of rock and fluid, V_{tot}, equation (12) can be written as

$$\frac{M_f}{\rho_f V_{tot}} + \frac{S_m^{\infty}}{\rho_m V_{tot}} = 1 \tag{13}$$

Note that V_{tot} changes if S_m^{∞} changes because

$$V_{tot} = \frac{M_f}{\rho_f} + \frac{S_m^{\infty}}{\rho_m} \tag{14}$$

Substituting (14) into (13) gives an expression for ϕ as a function of S_m^{∞}

$$\phi = \frac{M_f}{\rho_f \left(\frac{M_f}{\rho_f} + \frac{S_m^{\infty}}{\rho_m} \right)} \tag{15}$$

If the mineral mass S_m^{∞} is scaled by F_m, the scaling factor F^* for porosity, ϕ, can be calculated as

$$F^* \phi = \frac{M_f}{\rho_f \left(\frac{M_f}{\rho_f} + \frac{F_m S_m^{\infty}}{\rho_m} \right)} \tag{16}$$

Substituting (15) into (16), recognizing that the fluid volume V_f is $V_f = M_f/\rho_f$ and the solid volume V_m is $V_m = S_m^{\infty}/\rho_m$, and solving for F^* gives

$$F^* = \frac{V_f + V_m}{V_f + F_m V_m} \tag{17}$$

Equation (17) shows that if the mineral mass S_m^{∞} is scaled by the factor F_m, time, t, in the similarity variable η (equation 7) scales as the factor F^*, which is a function of F_m, the volume of the fluid V_f and mineral V_m. However, the similarity

variable also shows that scaling the distance x by division by the square root of F^* is equivalent to scaling time by multiplication by F^*.

The scaling factor F^* in (17) displays three interesting properties in the limits of $\phi \rightarrow 0$, $\phi \rightarrow 1$, and $F_m \rightarrow 0$. For very low water-rock ratios, i.e., $\phi \rightarrow 0$, the scaling factor F^* has the limit $1/F_m$, meaning that time in the similarity variable scales with the inverse of the scaling factor of the mineral mass. For very high water-rock ratios $\phi \rightarrow 1$, the scaling factor F^* has the limit 1, meaning that time in the similarity variable does not scale at all. If the scaling factor F_m decreases, i.e., $F_m \rightarrow 0$, the scaling factor for time F^* has the limit $1/\phi$, meaning that the maximum factor by which the efficiency of a simulation can be increased is the inverse of the porosity.

The behavior of F^* in the limit of $F_m \rightarrow 0$ suggests that it is not necessary to decrease F_m to a very small value. Obviously, F_m cannot be decreased without bound. The limit for decreasing F_m is given by the requirement of the quasi-stationary state approximation that the solute concentration is always much smaller than the mineral concentration (Lichtner, 1988; 1991). Using the notation given above and defining a bulk mineral density per unit volume ρ_{mV} as $\rho_{mV} = S_m / V_{tot}$, the requirement is given by the inequality

$$\frac{\Delta C}{\rho_{mV}} << 1 \qquad (18)$$

where ΔC is the difference in concentration between the concentration in equilibrium with the mineral C_{eq} and the concentration at the boundary C_o. The

behavior of F^* in the limit of $F_m \rightarrow 0$ (equation 17), however, shows that decreasing F_m to very small values does not increase the efficiency of the simulations, because F^* asymptotically reaches the value $1/\phi$.

II.4.2 Example Hydrothermal Alteration of Microcline to Muscovite

A simple reactive transport simulation of sericite replacing microcline using scaled and unscaled initial mineral masses and two different time-steps is shown in Figure 1. The time-step in graph (a) is ten times smaller than in graph (b). The same physical parameters and input conditions were used in both simulations. The initial mineral mass of microcline was scaled by the factor $F_m = 0.1$ in the second simulation for both time-steps. The time for the second simulation was scaled by the factor $F^* = 1.63$ according to (17) to match the results of the first simulation for both time-steps. Chemical reactions occurred under transport-limited conditions in all simulations.

The graph shows that the locations of the microcline and muscovite reaction fronts for the scaled and unscaled simulations are offset for both time-steps. The simulations using scaled mineral masses show faster dissolution of microcline and faster precipitation of muscovite. The microcline dissolution front advanced farther in the simulation using scaled masses than in the simulation using unscaled masses.

Using different time-steps also leads to different locations of the reaction fronts for the simulations with scaled and unscaled mineral masses, respectively.

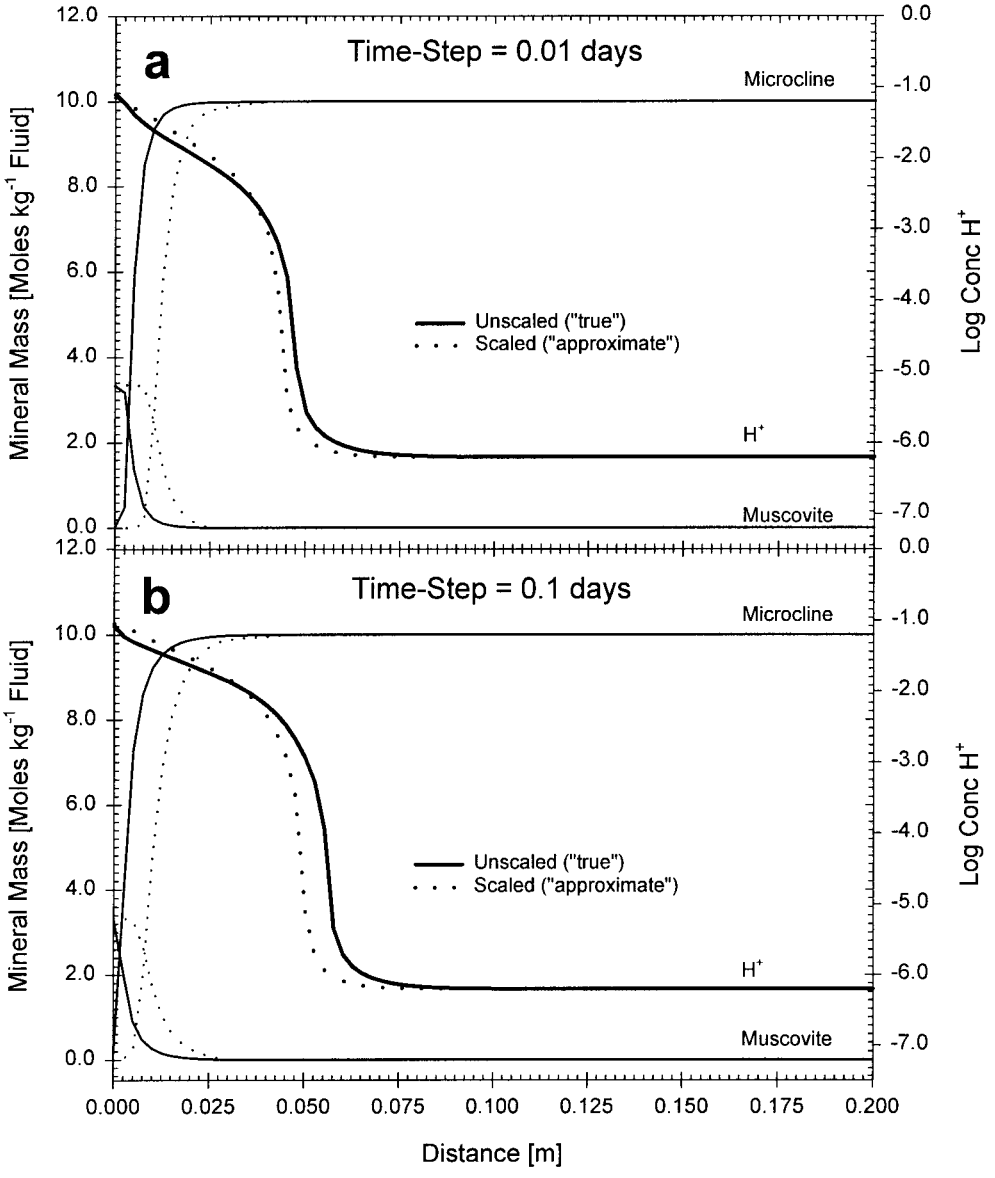

Figure II.1. Reactive transport simulation of muscovite replacing microcline at 400°C and 100 MPa after 40 days using scaled and unscaled mineral masses. The time-step for both scaled and unscaled simulations depicted in (a) was ten times smaller than in the simulations in (b). The bold lines show the results of unscaled initial mineral masses, while the dotted lines depict the results of scaled initial mineral masses. Solute transport was purely diffusive and reactions occurred under transport-limited conditions. Physical parameters and boundary conditions were identical for both simulations.

The simulations using a large time-step (Fig. 1b) yield mineral reaction fronts that are less developed than the mineral reaction fronts from simulations using a small time-step (Fig. 1a). The mineral reaction fronts of the simulation using unscaled mineral masses and small time-steps advanced further than the mineral reaction fronts of the simulation using unscaled mineral masses and large time-steps. The pH fronts in the simulations using scaled mineral masses are identical for both time-steps. The pH fronts in the simulations using unscaled mineral masses, however, are not identical for both time-steps (Fig. 1).

Using simulations with identical parameters but scaled mineral masses, unscaled mineral masses, and different time-steps leads to different location of reaction fronts and different time frames for the evolution of reaction fronts. This suggests inaccuracy in the model that is caused by the decoupling of the reaction and transport steps in the SIA method. The numerical error is also increased because quasi-stationary state is not fully reached in the reaction step. Using smaller time-steps increases the number of reaction steps and leads to faster mineral reactions that are closer to quasi-stationary state. Decreasing the time-step infinitely and calculating the reactions for quasi-stationary state would therefore reduce the numerical error.

The numerical error in the SIA method causes difficulties in calculating an absolute time and location of a reaction front. However, the relative location of the mineral reaction front in a sequence of reaction fronts is not changed. This means that only an approximate location and time frame for the evolution of a sequence of

reaction fronts can be calculated, but the relative location and the relative temporal evolution of sequence of reaction fronts is not affected by the numerical error.

The absolute time scale for the evolution of a sequence of reaction fronts is also dependent on several physical and chemical parameters, such as surface areas of minerals and concentration gradients of solutes, that are often difficult to estimate (e.g., Steefel and Lichtner, 1994). Calculating an absolute time and location of a reaction front is currently difficult in reactive transport simulations of fossil hydrothermal systems because of numerical problems and the uncertainties in some physical and chemical parameters.

As long as the criterion for the quasi-stationary state approximation (Lichtner, 1988; 1991) given in equation (18) is obeyed, scaling the initial mineral mass S_m^{∞} is a tool to carry out effective reactive transport simulations for geologic time in transport controlled systems. However, scaling initial mineral masses makes it even more difficult to calculate the absolute time frame of the evolution of reaction fronts.

II.5 Properties of Single-Component Systems

II.5.1 Exact Formulation for a Single Component System

As a simple example of a hypothetical chemical alteration front under quasi-stationary state conditions, consider the isothermal single-component system depicted in Figure 2. Dissolution of the mineral is pH-independent (i.e., it is not a

hydrolysis reaction), occurs at a constant rate, and is also strictly transport-limited. Solute transport is governed by diffusion only. Porosity and diffusivity are not changed significantly and diffusion is homogeneous. Solutes are transported away from the reaction front into a fracture where they are removed quickly by dispersion and advection. Under the assumption of fresh fluid as the boundary condition, the fluid within the fracture maintains a constant composition. The solute concentration in the fracture C_o is always much smaller than the concentration at the dissolution front C_{eq}. Diffusion reaches a quasi-stationary state after a short period of time because the mineral mass is large and the dissolution front moves slowly.

Analytical solutions for single component transport and reaction models have been derived and discussed by Lichtner (1985), Lichtner et al. (1986), Lichtner (1988), Novak et al. (1989), Lichtner (1991), and Lichtner and Balashov (1993). Solute transport processes in these derivations include both, advection and diffusion. In this section we will focus only on the analytical solutions that allow the prediction of the location and velocity of the reaction front $x_m(t)$.

Figure 2 shows that during quasi-stationary state, solutes are transported away from the dissolution front at the same rate as they are provided to the fluid at the reaction front. The boundary conditions are $C(t,0) = C_o$ in the fracture and $C(t,x) = C_{eq}$ in the matrix. The solute flux from the dissolution front to the fracture Ω_j decays as the square root of time and is approximately constant. The flux Ω_j can

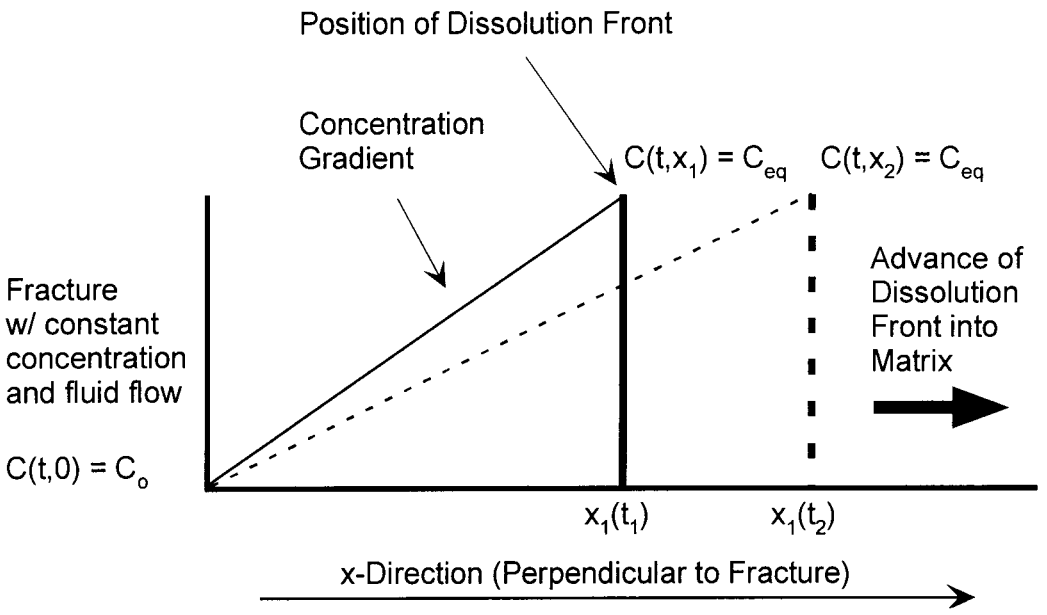

Figure II.2. Simplified physical model of a hydrothermal alteration front at quasi-stationary state showing the advance of a dissolution front and the response of the concentration gradient. The model is an isothermal single component system. Reactions are transport controlled. The location of the dissolution front is shown for two different times, $x_1(t_1)$ (bold line) and $x_1(t_2)$ (dashed line), respectively. The constant concentration boundary conditions are C_o in the fracture and C_{eq} at the dissolution front. C_o has a much lower concentration than C_{eq}. Note that the concentration gradient decreases with increasing time.

mathematically be expressed in two different ways. First, in terms if the difference in concentration Ω_j^C as

$$\Omega_j^C = -D_p \phi \frac{\Delta C}{x_m(t)} \tag{19}$$

Secondly, as the change of dissolved mass due to the advance of the reaction front Ω_j^S

$$\Omega_j^S = \frac{dS_m}{A_\Omega dt} \tag{20}$$

where ΔC is the difference between the concentration at the dissolution front C_{eq} and the concentration in the fracture C_o. The change in solid mass after the dissolution front has advanced a distance $\Delta x_m(t)$ (i.e., $\Delta x_m(t) = x_2(t) - x_1(t)$) is dS_m/dt. The area over which the flux occurs is A_Ω. Combining equations (19) and (20) gives

$$\Omega_j^C = \Omega_j^S = \frac{dS_m}{A_\Omega dt} = -D_p \phi \frac{\Delta C}{x_m(t)} \tag{21}$$

The change in solid mass dS_m/dt can also be expressed in terms of the mineral bulk density ρ_{mV}, the area over which flux occurs A_Ω, and the difference in the location of the dissolution front $\Delta x_m(t)$, Equation (21) becomes then

$$\frac{dx_m(t)}{dt} = \phi \frac{D_p}{\rho_{mV}} \frac{\Delta C}{x_m(t)} \tag{22}$$

For the initial condition $C(0,x) = C_{eq}$, the location of the mineral reaction front $x_m(t)$ as a function of time at quasi-stationary state is

$$x_m(t) = \sqrt{\frac{2D_p\phi}{\rho_{mV}}\Delta C t} \qquad (23)$$

Equation (23) implies that the location of the reaction front increases with the square root of time. Note that equation (23) is similar to the expression given in equation (68) on page 152 in Lichtner (1988). Taking the derivative with respect to time in equation (23) also yields the velocity $v_m(t)$ with which the dissolution front moves under quasi-stationary state conditions

$$\frac{dx_m(t)}{dt} = v_m(t) = t^{-1/2}\sqrt{\frac{D_p\phi}{2\rho_{mV}}\Delta C} \qquad (24)$$

Note that in this formulation the velocity decreases with time. Lichtner (1988) has also given an analogue equation that includes reaction kinetics and allows the calculation of the velocity of the reaction front $v_k(t)$ for pure diffusion in a single component system

Steefel and Lichtner (1998) have derived the formulation for the geometry of an alteration zone along a discrete fracture at a single quasi-stationary state. This allows calculating the slope $\sigma_m(t) = x/z$ of a mineral reaction front along a discrete fracture oriented in z-direction. The slope $\sigma_m(t)$ is not a function of time for a single quasi-stationary state. However, in a transient formulation, the slope of the reaction front is $\sigma_m(t) \rightarrow \infty$ at early times, while the slope is $\sigma_m(t) \rightarrow 0$ at late times, because diffusion of solutes into the matrix occurs at a lower rate than advection of solutes in the fracture (e.g., Neretnieks, 1980).

II.5.2 Spatial and Temporal Evolution of a Single Reaction Front

The spatial and temporal evolution of a single reaction front along a discrete fracture under quasi-stationary state conditions is depicted in Figure 3. From (23) it follows that the location of the mineral reaction front advances as the square root of time if diffusion is the governing transport process (Fig. 3a), while the velocity of the mineral front decreases as the inverse of the square root of time (Fig. 3b). This is given by the fact that the difference in concentration ΔC, pore diffusivity D_p, and the bulk density ρ_{mV} are very nearly constant. Furthermore, it follows that the location of a mineral reaction front scales with the difference in concentration, i.e. if the boundary concentration (C_o in Figure 2) is far from equilibrium with the concentration in the pore fluid (C_{eq} in Figure 2), the reaction front moves proportionally faster.

At a single quasi-stationary state, the slope of a reaction front $\sigma_m(t)$ along a discrete fracture with orientation in z-direction is constant (Steefel and Lichtner, 1998). However, since the temporal evolution is described as a sequence of quasi-stationary states, a transient description of the slope $\sigma_m(t)$ yields a slope of infinity at early times and zero as time reaches infinity. This follows from the fact that the location of a reaction front advances with the square root of time. A location $x_{z2}(t)$ downstream the fracture will advance at a different rate than the location $x_{z1}(t)$ upstream the fracture (Fig. 3c), because the reacting fluid needs some time to

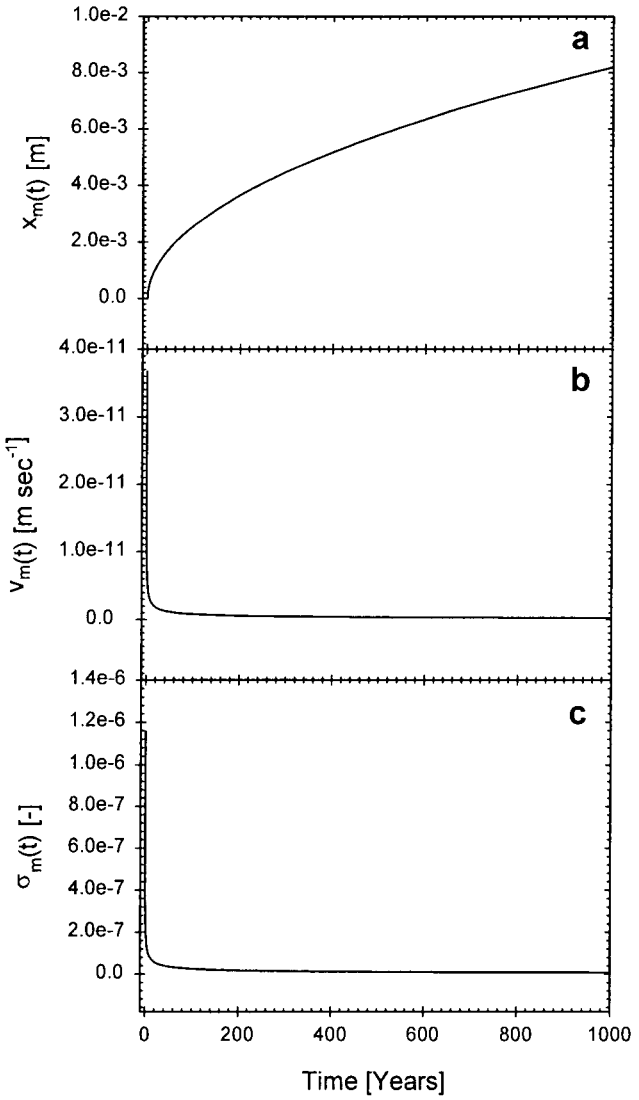

Figure II.3. Temporal evolution of location (a), velocity (b), and slope (c) of a quartz dissolution front at 400°C under quasi-stationary state conditions. Parameters used for the calculation are $D_p = 1.0 \times 10^{-10}$ m^2 s^{-1}, $\rho_{mV} = 2620$ kg m^{-3}, a_{SiO2} in equilibrium with quartz = 2.78×10^{-02} mole kg^{-1} (log K = -1.56), a_{SiO2} in the fracture = 0.001. The location of the dissolution front increases with the square root of time (a) while its velocity decreases with the square root of time (b). The slope of the front (c) has been calculated as the difference between two reaction front locations $x_{z1}(t)$ and $x_{z2}(t)$, respectively, along a discrete fracture. The locations are separated by the distance z = 100 m. The advance of the location front downstream of the fracture is delayed by the time t = f(z). Assuming that there is no dispersion and retardation of the solutes, $t = z/u_f$ with a Darcy velocity u_f of $u_f = 500$ m y^{-1}. The slope of the alteration front is infinity at early times and becomes zero at late times.

travel the distance z in the fracture. The observation that an alteration front along a fracture is parallel to the fracture only at late times explains why alteration envelopes usually pinch out downstream of the fracture.

II.6 Properties of Multi-Component Systems

II.6.1 Spatial and Temporal Evolution of Multiple Reaction Fronts

Predicting the spatial and temporal evolution of a sequence of mineral reaction fronts in a multi-component system is more difficult than predicting the evolution of a single mineral reaction front. The knowledge about the properties of the evolution of a single-component system, however, yields important understanding on how a multi-component system behaves. The equations derived by Lichtner (1988), Novak et al. (1989), Lichtner (1991), and Lichtner and Balashov (1993) also yield expressions that mathematically describe the spatial and temporal development of multiple mineral reaction fronts. The evolution of fossil hydrothermal alteration fronts can be studied using these equations, since transport processes are diffusion controlled and chemical reaction rates are high, i.e., local equilibrium can be assumed (c.f., Reed, 1997).

From the property of the similarity variable η (Equation 9) it follows that that the location of the reaction front in a multi-component system is determined by the concentration gradients of the involved aqueous species across an individual mineral reaction front (Equation 10). This also means that each mineral reaction

front can move with a different velocity $v_m(t)$, which is a function of the solute flux of the involved aqueous species across the mineral reaction front (Equation 11). Equation (11) also suggests that the velocities of a sequence of mineral reaction fronts are time-independent. Two important implications for the development of hydrothermal alteration fronts follow from this observation.

First, sharp reaction fronts border reaction zones upstream and downstream if reactions occur under transport controlled conditions (Lichtner, 1991). If the reaction fronts that bound a mineral reaction zone have different velocities, the width of a reaction zone (i.e., alteration halo) increases (Lichtner, 1991; Lichtner and Balashov, 1993). This is possible because in multi-component systems, the reaction front velocity is only a function of the solute flux across the reaction front, and the flux can vary across the upstream and downstream reaction front for an individual reaction zone. The ratio of the widths of two mineral reaction zones is constant because the reaction fronts bordering a mineral reaction zone move at a constant rate relative to each other (Fig. 4). Therefore, the widths of a series of hydrothermal alteration envelopes, each of them consisting of one ore more mineral reaction zones, increase with a constant ratio to each other. This allows the prediction of the evolution of the mineral assemblage once all reaction fronts have been established, because reaction fronts move at a known rate and the widths of reaction zones only increase with time. Furthermore, it follows from the discussion of the slope of a single reaction front along a discrete fracture, that hydrothermal alteration envelopes decrease in width along the fracture. The application for

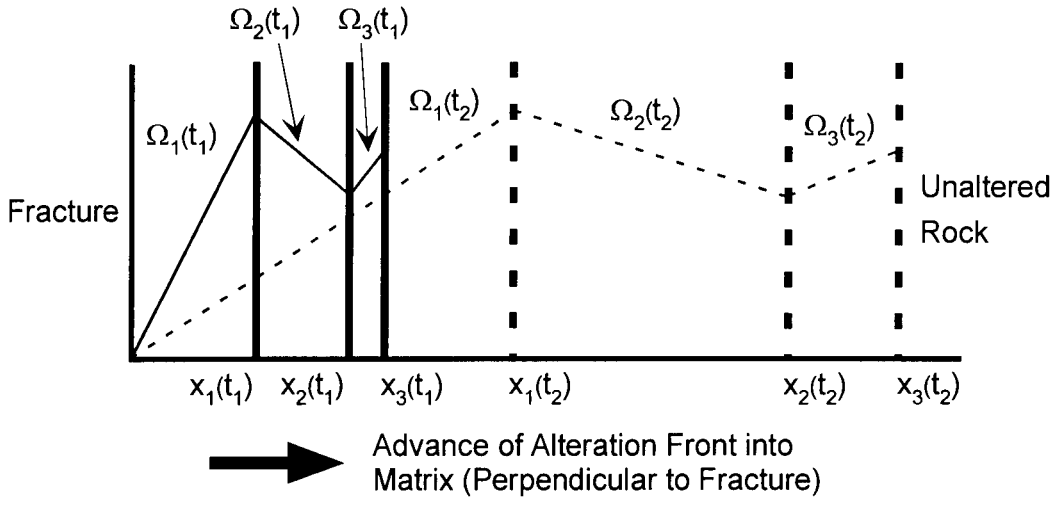

Figure II.4. Schematic representation of the spatial and temporal development of multiple reaction fronts $x_m(t)$. Each reaction front advances at an individual rate determined by the solute flux Ω_j across the reaction front. Note that the reaction fronts maintain their relative positions to each other and the ratio of their widths is constant at all times.

reactive transport modeling is that it is only necessary to solve for early times, i.e., until the complete pattern of reaction fronts has been developed. The sequence of mineral reaction fronts for all later times is then known, because mineral reaction zones only increase in width.

II.6.2 Hydrothermal Alteration at Butte, Montana

Two hydrothermal events are associated with the mineralization at the porphyry copper system at Butte, Montana: an early "pre-Main Stage" event and a late "Main Stage" event have formed in the 78 Ma Butte Quartz Monzonite (c.f., Meyer et al, 1968). Reed (1979) has classified the different hydrothermal alteration assemblages, and two types of alteration zones are very common within the pre-Main Stage alteration at Butte Montana. The first one is the "gray sericitic" (GS) alteration, where all feldspar, biotite, and amphibole of the host rock is altered to quartz, sericite and pyrite. The second one is the "sericite with remnant biotite" (SBr) zone, where feldspar and amphibole are altered to quartz, sericite and pyrite, but biotite is still present. The GS zone is found adjacent to the mineralized vein, while the SBr zone appears matrix inward. The occurrence of fresh feldspar marks the edge of unaltered host rock. Temperature and pressure for the alteration assemblage were about 400°C and < 100 MPa (Roberts, 1975; Oregon Butte Research Group, unpublished data). Reactive transport modeling has shown that the hydrothermal fluids that formed the alteration assemblages could have been

reducing, and comprised a low pH and low salinity (Geiger, 2000). The code CSP3D3.0 (Matthäi and Roberts, 1999) was applied to simulate reactive transport in of the hydrothermal alteration. Initial mineral masses were scaled in the simulation to model the system efficiently for longer time spans. See Geiger (2000) for a detailed discussion on the reactive transport simulation of the GS and SBr alteration at Butte, Montana.

Concentration profiles across the calculated mineral assemblages perpendicular to the fracture are depicted in Figure 5 to show the spatial and temporal evolution of the alteration zone between 10 and 30 years. Note that the times cannot be understood as absolute times due to the numerical inaccuracy in the SIA method explained above.

The mineral reaction fronts display a broad width, which is due to the decoupling of the reaction and transport step in the computational model. The plots clearly show that each mineral reaction front advances at a specific rate and mineral reaction zones increase with time. It appears as if the velocity of an individual reaction front decreases with time as predicted by equation (11). It is very difficult, however, to directly calculate a location or velocity for an individual reaction front because the system is not a single-component system anymore and a specific fluid-rock reaction involves several aqueous species. Further, the concentration gradients and fluxes of the aqueous species across the reaction front are non-linearly related to a series of other mineral reactions and change through time.

Figure II.5. Results of reactive transport simulations showing the spatial and temporal evolution between 10 and 30 years of the gray sericite (GS) and sericite with remnant biotite (SBr) alteration zones at the porphyry copper deposits at Butte, Montana. See Geiger (2000) for a detailed discussion on the setup of the simulation. Plots for the minerals comprising the host-rock and the alteration products are shown for 10 (a and e), 15 (b and f), 20 (c and g), and 30 years (d and h), respectively. Annite marks the transition between the GS and the SBr zone. Note that the mineral masses for quartz are scaled in the plots by a factor of 0.1.

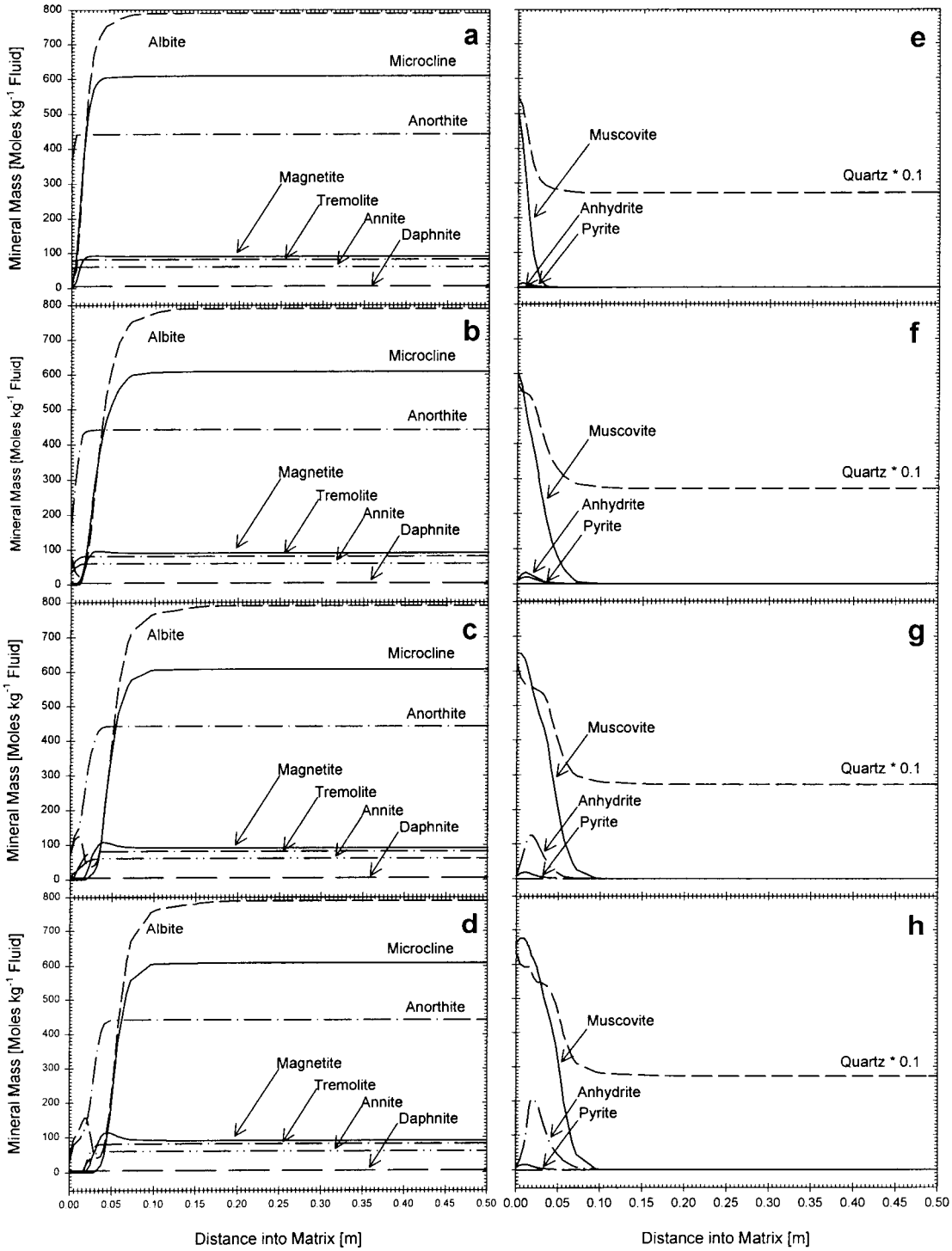
a
b
c
d
e
f
g
h
Albite
Microcline
Anorthite
Magnetite
Tremolite
Annite
Daphnite
Muscovite
Quartz * 0.1
Anhydrite
Pyrite
Mineral Mass [Moles kg-1 Fluid]
Distance into Matrix [m]
0
100
200
300
400
500
600
700
800
0.00
0.05
0.10
0.15
0.20
0.25
0.30
0.35
0.40
0.45
0.50

With the exception of magnetite, the relative locations of the mineral reaction fronts for the minerals comprising the host rock remain constant to each other. Reaction zones for the minerals comprising the host rock (not including magnetite) are from fastest to slowest reacting: Albite, microcline, tremolite, annite, anorthite, daphnite. Note that the slow dissolution of anorthite is possibly an artifact due to an error in the thermodynamic database and that the anorthite front would probably lead all other dissolution fronts with the correct reaction rate. Daphnite is stable at the given conditions. The magnetite reaction front leads all other reaction fronts at early time, but its advance decreases at the fastest rate and the front is almost stable in position at late time. The mineral reaction zones of the alteration products muscovite, anhydrite, and quartz increase with time because their precipitation fronts advance at individual rates that are closely related to the rate of advance of the dissolution fronts of the minerals comprising the host rock.

Similar to the dissolution fronts of the minerals comprising the host-rock, the relative locations of the precipitation fronts of the alteration products remain constant to each other. The width of the pyrite zone, however, appears to be almost constant through time (the leading edge of the pyrite zone is located at approximately 0.05 m), which is probably related to the unusual fast decrease in the advance of the magnetite dissolution front. The spatial stability of the pyrite zone suggests that this zone could be understood as a ghost zone applying the terminology of Lichtner and Balashov (1993).

An important conclusion follows from the observation that the relative locations of all reaction fronts are constant to each other. Considering that the anorthite front probably dissolves at a higher rate, the annite dissolution front trails all other reaction fronts and therefore always marks the transition of the GS to SBr zone because the pattern of mineral reaction fronts remains constant through time. The annite reaction zone starts to migrate into the matrix after approximately 25 years, which forms the GS zone adjacent to the fracture. The width of the GS zone increases because the annite dissolution front continues to advance deeper into the matrix, so does the width of the SBr zone because the feldspar dissolution front, which leads all reaction fronts, continues to advance deeper into the matrix.

The initial mineral masses have been scaled in the simulation. This allowed an efficient simulation for long time spans. A smaller time-step could be applied which reduced the error of unrealistically wide reaction fronts introduced by the decoupling of the transport and reaction step via the SIA method in CSP3D3.0. An infinitely small time-step would allow to model sharp reaction fronts as required by the assumption that reactions are transport controlled and observed in the natural samples (c.f., Fig. 2).

II.7 Concluding Remarks

Three points have been discussed in this paper. First, scaling the initial mineral mass is an effective method to simulate multi-component diffusion and reaction in decoupled reactive transport models if reactions occur under transport

controlled conditions and the requirement for the quasi-stationary state assumption are obeyed (i.e., solute concentrations are always smaller than mineral concentrations). The mass-scaling properties can be directly studied from the similarity variable η. If the mineral mass is scaled by a factor F_m, time must be scaled by the factor F^*, which is a function of F_m, the volume of the fluid V_f and the mineral V_m. Scaling distance by the square root of F^* is also equivalent to scaling time by F^*. Mass scaling, however, increases the numerical inaccuracy in the simulations because the locations of mineral reaction fronts to each other appear to be incorrect although the relative locations of mineral reaction fronts are not affected. Furthermore, the absolute time necessary to establish the full sequence of reaction fronts cannot be determined exactly. The decoupling of the reaction and transport steps probably causes this numerical problem, because changing the time-steps in the simulation that otherwise use identical parameters also yields different locations for the reaction fronts and different time frames for the evolution of the reaction fronts. This makes the application of the SIA method currently problematic for reactive transport simulations of geologic systems. However, many physical and chemical parameters in fossil hydrothermal systems are not well known and may introduce a bigger uncertainty than the numerical inaccuracy of the SIA method.

Secondly, quantitative descriptions of the evolution of mineral reaction fronts that have been derived recently by Lichtner (1988), Novak et al. (1989), Lichtner (1991), Steefel and Balashov (1993), and Steefel and Lichtner (1998) were

compiled in this paper. These descriptions, which mainly derive from the properties of the quasi-stationary state assumption (Lichtner, 1988; 1991), allow to quantitatively assess the spatial and temporal development of mineral reaction fronts in hydrothermal systems.

Reaction fronts ideally have zero width under transport controlled conditions which explains the sharp transition from the alteration zone to the fresh rock. In a multi-component system, the velocity of an individual reaction front is largely time-independent and also a function of the concentration gradient and solute flux across the particular front. In a multi-component system, the reaction fronts therefore maintain their relative position to each other once a pattern of precipitation and dissolution fronts in a hydrothermal alteration zone has been established. Mineral reaction zones usually grow with increasing time as their bordering reaction fronts advance at a calculable rate. In theory, this allows to only simulate the fully developed pattern of reaction fronts for one time, because it can be predicted how the pattern will evolve at later times. The slope of an alteration front along a fracture is infinity at early times and reaches zero at late times because advection in the fracture occurs at a higher rate than diffusion in the rock matrix. Reaction zones downstream along the fracture therefore have narrower widths and tend to pinch out.

Thirdly, the derived properties for the spatial and temporal evolution of multiple reaction zones can be applied to better understand the results of reactive transport simulations of hydrothermal reactions in terms of their spatial and

temporal evolution. However, a strict quantitative assessment of the results is difficult because concentration gradients are a non-linear function of multiple aqueous and solid reactions. Further, decoupled reactive transport models tend to calculate widths of reaction zones that are broader than observed in natural samples.

II.8 Acknowledgements

We are greatly indebted to Carl Steefel of the Lawrence Livermore National Laboratory for his interest, help, and fruitful discussions during the course of this work. The first author would also like to thank the Radiation Center at Oregon State University, especially Erwin Schütfort and Steve Binney, for the financial support throughout this Masters thesis. Financial support for the geologic studies at Butte was supported by the National Science Foundation, grant NSF-EAR-9614683.

II.9 References

Geiger, S., 2000, Reactive transport modeling in discrete fractures: Applications to the formation of sericitic hydrothermal alteration at Butte, Montana. MS Thesis, Dept. of Geosciences, Oregon State University, 124 pages.

Lichtner, P.C., 1985, Continuum model for simultaneous chemical reactions and mass transport in hydrothermal systems. Geochimica et Cosmochimica Acta, v. 49, 779-800.

Lichtner, P.C., Oelkers, E. H., and Helgeson, H.C., 1986, Interdiffusion with multiple precipitation / dissolution reactions: Transient model and steady-state limit. Geochimica et Cosmochimica Acta, v. 50, 1951-1966.

Lichtner, P.C., 1988, The quasi-stationary state approximation to coupled mass transport and fluid-rock interaction in a porous medium. Geochimica et Cosmochimica Acta, v. 52, 143-165.

Lichtner, P.C., 1991, The quasi-stationary state approximation to fluid/rock interaction: local equilibrium revisited. In: Ganguly, J. (ed.) Diffusion, atomic ordering and mass transport. Advances in Physical Geochemistry, v. 8, 454-562. Springer Verlag.

Lichtner, P.C., 1993, Scaling properties of time-space kinetic mass transport equations and the local equilibrium limit. American Journal of Science, v. 293, 257-296.

Lichtner, P.C. and Balashov, V.N., 1993, Metasomatic zoning: appearance of ghost zones in the limit of pure advective mass transport. Geochimica et Cosmochimica Acta, v. 57, 369-387.

Matthäi, S.M. and Roberts, S.G., 1999, Complex system platform CSP3D3.0 user's guide. Swiss Federal Institute of Technology (ETH) Zurich, 106 pages.

Meyer, C., Shea, E.P., Goddard, C.C., and staff, 1968, Ore deposits at Butte, MT. in Ridge, D. J. (ed.) Ore deposits of the United States 1933-1967 (Graton-Sales Vol.): v. 2, 1363-1416.

Neretnieks, I., 1980, Diffusion in the rock matrix: an important factor in radionuclide retardation? Journal of Geophysical Research, v. 85, 4379-4397.

Novak, C.F., Schechter, R.S., and Lake, L.W., 1989, Diffusion and solid dissolution/precipitation in permeable media. AIChE Journal, v.35, 1057-1072.

Reed, M.H., 1979, Butte District Early Stage Geology. Anaconda Company report, 40 pages., 24 plates and figures.

Reed, M.H., 1997, Hydrothermal alteration and its relationship to ore fluid composition. In: Barnes, H.L. (ed.), Geochemistry of hydrothermal ore deposits, 3rd edition, 303-365. John Wiley & Sons.

Reed, M.H., 1998, Calculations of simultaneous chemical equilibria in aqueous-mineral-gas systems and its application to modeling hydrothermal processes. In: Richards, J.P. and Larson, P.B. (eds.), Techniques in hydrothermal ore deposits geology. Reviews in Economic Geology, v. 10, 109-124.

Roberts, S.A., 1975, Early hydrothermal alteration and mineralization in the Butte district, Montana. Unpublished Ph.D. thesis, Harvard University.

Steefel, C. I. and Lasaga, A. C., 1994, A coupled model for transport of multiple chemical species and kinetic precipitation / dissolution reactions with application to reactive flow in single phase hydrothermal systems. American Journal of Science, v. 294, 529-592.

Steefel, C.I. and Yabusaki, S.B., 1996, OS3D/GIMRT, Software for Multicomponent-Multidimensional Reactive Transport, Users Manual and Programmer's Guide. PNL-11166, Pacific Northwest Laboratory, Richland, Washington.

Steefel, C.I. and Lichtner, P.C., 1998, Multicomponent reactive transport in discrete fractures: I. Controls on reaction front geometry. Journal of Hydrology, v. 209, 186-199.

Valocchi, A.J. and Malmstead, M., 1992, Accuracy of operator splitting for advection-dispersion-reaction problems. Water Resources Research, v. 28, 1471-1476.

Yeh, H.C. and Tripathi, V.S., 1989, A critical evaluation of recent developments in hydrogeochemical transport models of reactive multichemical components. Water Resources Research, v. 25, 93-108.

Yeh, H.C. and Tripathi, V.S., 1991, A model for simulating transport of reactive multispecies components: Model development and demonstration. Water Resources Research, v. 27. 3075-3094.

Zysset, A. and Stauffer, F., 1992, Modeling of microbial processes in groundwater infiltration systems. In Russell, T.F., Ewing, R.E., Brebbia, C.A., Gray, W.G., and Pinder, G.F. (eds.): Mathematical Modelling in Water Resources. Computational Mechanics Publications, Billerica, Massachusetts.

Zysset, A., Stauffer, F, and Dracos, T., 1994, Modeling of chemically reactive groundwater transport. Water Resources Research, v. 30, 2217-2228.

CHAPTER III

THE EVOLUTION OF THE EARLY HYDROTHERMAL ALTERATION AT BUTTE, MONTANA: NEW INSIGHTS FROM REACTIVE TRANSPORT MODELING

Sebastian Geiger [†], Roy Haggerty, John H. Dilles

Department of Geosciences, Oregon State University, Wilkinson Hall,

Corvallis, OR 97331-5506, U.S.A

Mark H. Reed

Department of Geological Sciences, 1272 University of Oregon,

Eugene, OR 97403-1272, U.S.A

Stephan K. Matthäi

Department of Earth Sciences, Swiss Federal Institute of Technology (ETH),

NO Building, Sonneggstr. 32, CH-8092 Zurich, Switzerland

[†] Corresponding author: e-mail, Sebastian.Geiger@orst.edu

To be submitted to Economic Geology

III.1 Abstract

Reactive transport modeling of hydrothermal alteration of a rock matrix bordering a discrete vein channel suggests that the gray sericitic and sericite with remnant biotite alteration envelopes at the porphyry copper deposit at Butte, Montana, can be formed by a reducing, low pH, and low salinity fluid at about 400°C and less than 100 MPa during a time span of approximately one hundred years or less. Hydrothermal alteration has little effect on the porosity of the host-rock (Butte Quartz Monzonite), and the diffusivity also changes little. A sequence of mineral reaction fronts characterizes the alteration envelopes. The biotite dissolution front occurs closest to the vein channel and marks the transition from the gray sericitic to sericite with remnant biotite envelope. The plagioclase dissolution front occurs farthest into the matrix and marks the edge of relatively fresh Butte Quartz Monzonite. From the properties of the quasi-stationary state approximation (Lichtner, 1988; 1991), it follows that once the sequence of reaction fronts is fully established, their relative locations remain constant and the widths of the reaction zones increase with the square root of time. The widths of the reaction zones decrease along the fracture the rate of diffusion of reactive solutes in the rock matrix is slower than the rate of advection of the reactive solutes in the fracture.

III.2 Introduction

In the porphyry copper district at Butte, Montana, successions of hydrothermal alteration envelopes border veins within the Butte Quartz Monzonite host-rock (Sales and Meyer, 1948; Sales and Meyer, 1949; Meyer et al., 1968). The mechanism that forms hydrothermal alteration zones along fractures is a combination of the transport of fluid, solutes, and heat in a fracture within the geologic medium, the exchange of heat and solutes between the fracture and the bordering rock matrix, and the chemical interaction of the solutes with the solid phase (c.f., Steefel and Lasaga, 1994; Steefel and Lichtner, 1994; Reed, 1997; Steefel and Lichtner, 1998a, 1998b). These interactions usually involve diffusion, advection, and dispersion of heat and solutes, and precipitation and dissolution of minerals. The spatial and temporal changes of the physical and chemical properties of the fluid and the geologic medium are strongly connected, often resulting in significant feedback between solute transport and chemical reactions (e.g., Lichtner, 1996; Steefel and MacQuarrie, 1996). Combining the physics of solute and heat transport with the chemistry of the water-rock interactions is commonly called "reactive transport".

Although many important advances in the physics of reactive transport have been made during recent years (e.g., Lichtner, 1985; Lichtner et al., 1986; Lichtner, 1988; Yeh and Tripathi, 1989; Yeh and Tripathi, 1991; Engesgaard and Kipp, 1992; Lichtner 1992; Steefel and Lasaga, 1992; Valocchi and Malmstead, 1992; Zysset and Stauffer, 1992; Lasaga and Rye, 1993; Lichtner, 1993; Lichtner and

Balashov, 1993; Steefel and Lasaga, 1994; Zysset et al., 1994; Steefel and Lichtner, 1998a), applications to multi-component transport and reaction modeling have mostly been limited to natural systems with temperatures below 100°C (e.g., Lichtner and Biino, 1992; Steefel and Lichtner, 1994; Glynn and Brown, 1996; Brown et al., 1998; Soler and Lasaga, 1998; Steefel and Lichtner, 1998b). The difficulties in applying reactive transport modeling to high temperature environments, such as active or fossil hydrothermal systems, arise from the mathematical complexity of the problem, uncertainties in the physical and chemical parameters, sparse field data, and the large amount of computing time required to simulate sufficient geologic time.

Only a few studies have quantitatively assessed the coupling of transport processes and geochemical reactions in hydrothermal environments. Simulations of hydrodynamic flow, heat transfer, and coupled isotope exchange were carried out by Norton and Taylor (1979) for the Skaergaard intrusion and by Cathles (1983) for Kuroko-type massive sulfide deposits. Wells and Ghiorso (1991) studied the dissolution and precipitation of quartz in mid-ocean ridges. Phillips (1991) discussed an application of the fundamentals of transport and reaction in a hydrothermal system to a dolomitized reef complex. Steefel and Lasaga (1992; 1994) presented two-dimensional simulations of multi-component reactive transport in hydrothermal systems and the feedback of chemical effects on fluid mixing and reaction-induced permeability-porosity changes. Johnson et al. (1998) modeled quartz and tuff dissolution at elevated temperatures in a plug-flow reactor.

Beaudoin and Therrien (1999) simulated oxygen isotope exchange in three dimensions for the Kokanee Range silver-lead-zinc vein field in Canada. He et al. (1999) presented a one-dimensional reactive transport model for the alteration of the Tongchang porphyry copper deposit in China.

Simulations of wall-rock alteration at low temperatures were carried out recently by Steefel and Lichtner (1994) and Steefel and Lichtner (1998b), who applied multi-component reactive transport modeling to the chemical alteration of marls bordering a fracture filled with hyper-alkaline fluid. Those simulations show a significant negative feedback between reactions and transport over the time span of tens of years. Precipitation of alteration minerals causes the porosity of the rock matrix to decrease and slows the transport between the fracture and the host-rock.

Three main points that are related to the development of high-temperature hydrothermal alteration zones are addressed in this paper. First we study the spatial and temporal evolution of the succession of the hydrothermal alteration fronts and the feedback between solute transport and mineral reactions. The key question that is addressed in this point is how the individual mineral reaction fronts advance in the rock matrix. Secondly, we give an approximate time frame necessary to form the observed alteration halos. Lastly, we study the characteristics of the hydrothermal fluid that has generated the known alteration. In contrast to active low-temperature hydrothermal environments, it is usually difficult to sample active high-temperature hydrothermal fluids and obtain information about the composition of the hydrothermal fluid in high-temperatures fossil systems, and

reactive transport modeling is therefore a good tool to calculate an approximate composition of the reacting fluid.

The petrology of the early hydrothermal alteration systems at Butte is well-studied (e.g., Sales and Meyer, 1948; Sales and Meyer, 1949; Meyer et al., 1968; Brimhall, 1977; Reed, 1979), and some of the alteration types at Butte (i.e., the sericitic pre-Main Stage type) are common in many porphyry copper deposits (c.f., Lowell and Guilbert, 1970; Gustafson and Hunt, 1975; Dilles and Einaudi, 1992). Therefore, the early hydrothermal alteration offers a good example for reactive transport modeling of a fossil high-temperature hydrothermal system.

In this paper, we use a numerical multi-component reactive transport model and apply the object-oriented finite element C++ code CSP3D3.0 (Matthäi and Roberts, 1999) to simulate the spatial and temporal development of two of the most prevalent early hydrothermal alteration assemblages at Butte, i.e., the gray sericitic and sericite with remnant biotite alteration of the sericitic pre-Main Stage type. In the approach here, we directly simulate one-dimensional transport and reaction of vein fluid components with the adjacent porous wall-rock; the application of previous models allows the extension of the one-dimensional model to a two-dimensional model that involves fluid flow and solute transport via advection in the vein-channel.

We also attempt to calculate an approximate composition of the hydrothermal fluid that has formed the characteristic assemblages.

III.3 Geological Background

III.3.1 Geology of the Butte District

The general geology of the Butte district is depicted in Figure 1. The Butte district is located in the 76 Ma Butte Quartz Monzonite, the central and volumetrically dominant pluton of the 74 to 78 Ma Boulder Batholith (Knopf, 1957; Klepper, 1973; Smedes, 1973; Martin et al., 1999). The Butte Quartz Monzonite is coarse-grained and compositionally uniform throughout the Butte district. Plagioclase, quartz, potassium feldspar, biotite, hornblende, magnetite, and titanite are the principal minerals of the Butte Quartz Monzonite (Smedes, 1977). Table 1 shows the bulk composition of fresh Butte Quartz Monzonite from the Butte district. Alteration, mineralization, and metal enrichment in the Butte district are associated with vein sets of different ages and orientations through which hydrothermal fluids flowed. Ore minerals occur in either the veins or in the surrounding alteration envelope (Sales and Meyer, 1948; Sales and Meyer, 1949; Meyer et al., 1968). An early porphyry Cu-Mo "pre-Main Stage" is followed by the Butte "Main Stage" of large, through-going fissure-veins containing Cu-Fe-Zn-Pb-As-Ag-Mn mineralization (Meyer et al., 1968).

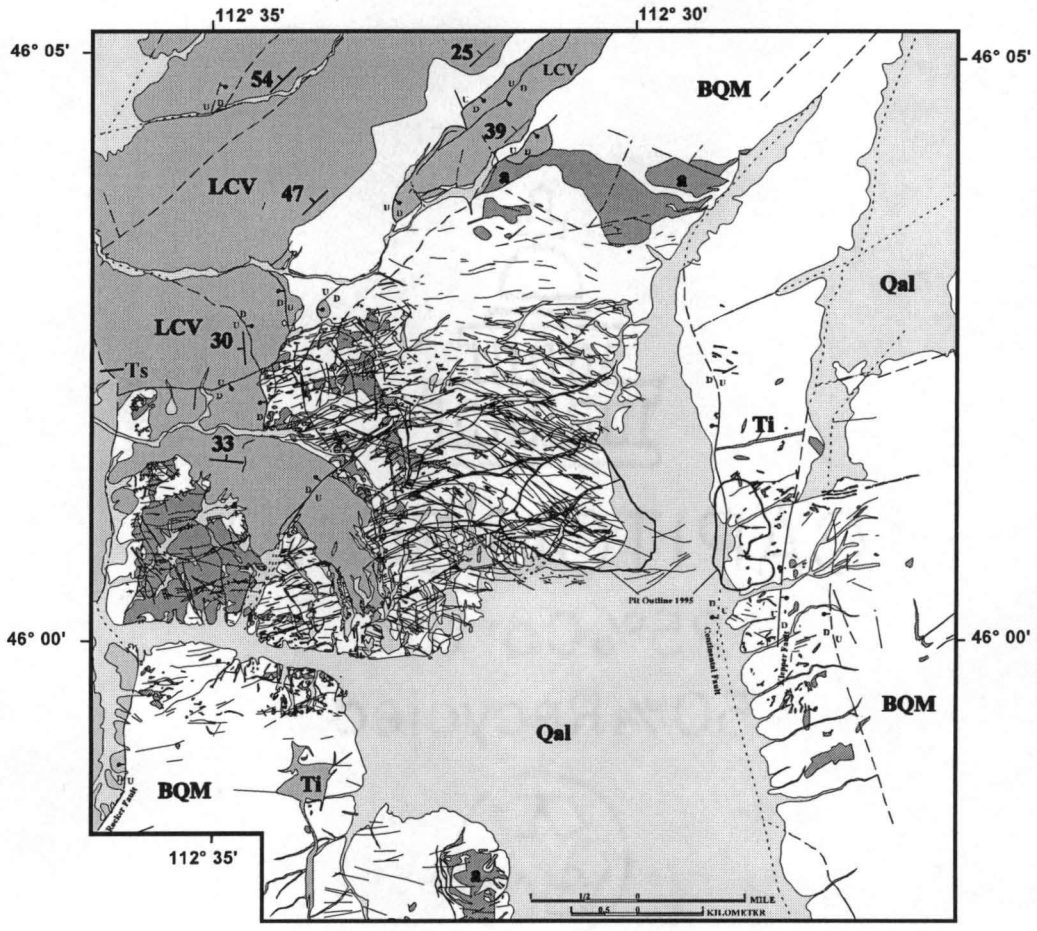

Figure III.1. Generalized geologic map of the Butte District (compilation of Houston, 1999, with geology from Proffett, 1973; Houston, 1999; G.H. Burns and others of the Anaconda company). The Butte district lies in southwestern Montana within a series of plutons that together form the 74 to 78 Ma Boulder Batholith. The 76 Ma old Butte Quartz Monzonite (BQM) is the volumetrically largest intrusion of the Boulder Batholith and is host of the mineralization at Butte. The BQM is coarse grained and has a uniform mineralogy of plagioclase, quartz, potassium feldspar, biotite, hornblende, magnetite, and titanite. The BQM is cut by aplite, granoaplite, and pegmatite (a) dikes and sills, and by quartz porphyry dikes that are in turn cut by mineralized veins Post dating the ores are rhyodacite and rhyolite dikes (Ti), Lowland Creek Volcanics (LCV), clastic sediments (Ts), and alluvian (Qal). Early porphyry Cu-Mo mineralization is being exploited in the Continental Pit and underlies the Berkeley Pit at 1000 m below the surface. Younger, Main Stage Cu-As-Zn-Pb-Ag veins (plotted) were mined in the Berkeley Pit area, and to the west and northwest.

Oxide	wt %
SiO_2	64.92
Al_2O_3	15.46
Fe_2O_3	1.81
FeO	2.70
MgO	2.05
CaO	4.24
Na_2O	3.06
K_2O	3.94
TiO_2	0.53
P_2O_5	0.18
MnO	0.09
H_2O^+	0.59
H_2O^-	0.12
CO_2	0.06
BaO	0.09
SO_3	0.05

Table III.1. Chemical Composition of the Butte Quartz Monzonite (Analysis after Smedes, 1973)

III.3.2 Hydrothermal Systems and Alteration Assemblages

High-temperature hydrothermal fluids were introduced into fractures within the Butte Quartz Monzonite where they chemically altered the fresh rock to form alteration envelopes (Meyer et al., 1968; Brimhall, 1977). Two hydrothermal events can be distinguished at Butte: an early "pre-Main Stage" event and a late "Main Stage" event, possibly similar in age or more likely separated by as much as 12 Ma (Meyer et al., 1968; Martin et al., 1999; Snee et al., 1999).

The pre-Main Stage mineralization is composed of three principal substages distinguished by vein cutting relations and distinct alteration. From early to late

these stages are: (1) Cu-bearing veinlets with biotitic alteration envelopes, (2) quartz-molybdenite veinlets, largely lacking alteration, and (3) pyrite-quartz veinlets with envelopes of sericitic alteration. The early biotitic or K-silicate alteration is centered in the district on a series of biotite breccias and contemporaneous quartz-porphyry dikes that cut the Butte Quartz Monzonite (Meyer et al., 1968). The "early dark micaceous" veinlets are less than 3 cm wide with alteration envelopes that are 1 to 30 cm wide (Brimhall, 1977). The alteration halos on these veinlets consist of alkali feldspar, quartz, muscovite, anhydrite, andalusite, biotite, corundum, pyrite, chalcopyrite, and magnetite (e.g., Brimhall, 1977).

The sericitic alteration bordering the pyrite-quartz veins of the third substage is the subject of modeling presented in this paper. Such alteration is also typical for many other porphyry deposits around the world (c.f., Lowell and Guilbert, 1970; Gustafson and Hunt, 1975; Dilles and Einaudi, 1992). This Butte pre-Main Stage sericitic alteration is characterized by two different mineral assemblages (Reed, 1979). The innermost zone (~ 1cm wide) is gray sericitic, wherein all feldspar, biotite, and amphibole of the Butte Quartz Monzonite has been altered to muscovite, quartz, and pyrite. The outer zone (~ 0.5 cm wide) contains sericite with remnant biotite, wherein feldspar and amphibole are altered to sericite, quartz, and pyrite, but much of the primary biotite remains. In most sericitic samples in the Butte district, the paired alteration envelopes are developed in Butte Quartz Monzonite in which hornblende was previously altered to biotite

during the early K-silicate alteration stage. A typical example of a pyrite-quartz vein with gray sericitic and sericite with remnant biotite zones is shown in Figure 2.

The Main Stage hydrothermal event produced the low-temperature sericite-kaolinite-montmorillonite alteration described by Meyer et al. (1968). Brimhall (1979; 1980) and Brimhall and Ghiorso (1983) proposed that input of new magmatic fluids leached pre-Main Stage copper and formed the extensive Main Stage copper mineralization. The Main Stage alteration selvages can be more than one meter wide and are typically zoned from local inner advanced argillic zones (quartz, sericite, dickite, alunite, kaolinite or pyrophyllite) to a prominent "white" sericite zone to outer zones where kaolinite and montmorillonite have replaced igneous plagioclase (Meyer et al., 1968).

Oxygen and hydrogen isotope evidence indicates a large meteoric component in the Main Stage fluids (Sheppard and Taylor, 1974), but recent studies show that magmatic fluids dominated the fluids that formed the gray sericitic alteration (Zhang et al., 1999). The salinities of the fluids of the sericitic pre-Main Stage alteration are approximately 1 to 2 wt. % NaCl (R.J. Bodnar, pers. comm., 1996). Limited fluid inclusion data from quartz samples from the pre-Main Stage veins indicate temperatures of 350°C to 400°C and pressures of less than 100 MPa for the gray sericitic alteration (Oregon Butte Research Group, unpublished data). Petrological studies (Roberts, 1975; Brimhall, 1977) indicate temperatures of 650 ± 50°C for the earlier pre-Main Stage types. Sulfur isotope equilibrium temperatures also suggest temperatures of 550 - 600°C (Zhang et al., 1999).

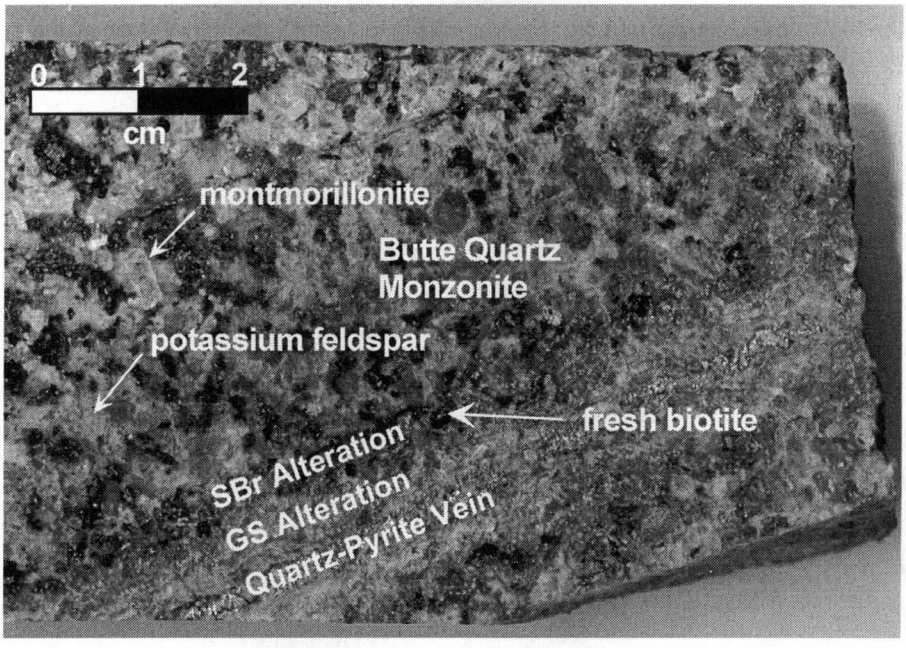

Fracture or Vein	GS Alteration	SBr Alteration	BQM
	ser, qtz, py, rare: anh, carb, ep	ser, qtz, bt, py, rare: anh, carb, ep	ksp, plag qtz, bt, mag

Figure III.2. Hydrothermal alteration sample from drill core 11148 at 984.5 ft depth showing the zonation of the sericitic pre-Main Stage alteration halos from the fracture into the matrix. Early K-silicate alteration has altered the hornblende of the Butte Quartz Monzonite (BQM) to secondary biotite. Younger hydrothermal fluids have altered the plagioclase in the BQM to montmorillonite. Note that the selvages parallel the vein and imply that diffusion occurred perpendicular to the vein channel. A 0.4 cm wide gray sericitic alteration zone (GS) is located adjacent to the quartz and pyrite vein (0.2 cm wide) and is characterized by alteration of feldspar, primary and secondary biotite to sericite, quartz, and pyrite. Minor amounts of anhydrite, epidote, and carbonates are rarely found in the gray sericitic alteration. The sericite with remnant biotite zone (SBr) (0.3 cm in width) is characterized by the occurrence of fresh biotite (black flakes in this sample), whereas feldspar of the BQM are still altered to sericite and quartz. The major disseminated sulfide in both sericitic zones is pyrite. The occurrence of fresh plagioclase marks the onset of unaltered BQM. Note the simple fractures (single breakage events) in the upper left, approximately 0.2 mm in width. These may record the aperture of the fracture while open to fluid flow. Mineral abbreviations are: ser, sericite; qtz, quartz; py, pyrite; an, anhydrite; carb, carbonate; ep, epidote; ksp, potassium feldspar; plag, plagioclase; mont, montmorillonite; bt, biotite.

For the pre-Main Stage and Main Stage events, respectively, Brimhall (1977) and Meyer et al. (1968) have discussed the diffusive transport of acidic high-temperature fluids perpendicular to the vein into the Butte Quartz Monzonite. The pH of the fluid increases along the diffusion path and a variety of alteration envelopes is formed parallel to the fracture, representing different stages of equilibrium mineral assemblages formed by interaction of the rock with the fluid, where the chemical composition of both the fluid and rock change with distance from the vein due to fluid-mineral reactions (Meyer et al., 1968; Brimhall, 1977).

III.4 Physical and Chemical Model of Hydrothermal Alteration Perpendicular to a Vein

The following physical model, which is similar to the one discussed by Reed (1997) and Steefel and Lichtner (1994; 1998b), is employed to simulate the evolution of the sericitic pre-Main Stage alteration zones. A low-permeability rock matrix borders a thin, single fracture (Fig. 3). The fracture represents what was once a two-dimensional fracture or vein channel that is now a mineral-filled veinlet, i.e., pyrite-quartz veinlets in the case of the gray sericite alteration. The width of the fracture when open is difficult to estimate, because open space is not preserved, but simple fractures are typically less than 0.5 mm wide (c.f., Fig. 2). Most veinlets record multiple fracture and vein-filling events to produce veinlets that are 1 mm to 2 cm wide.

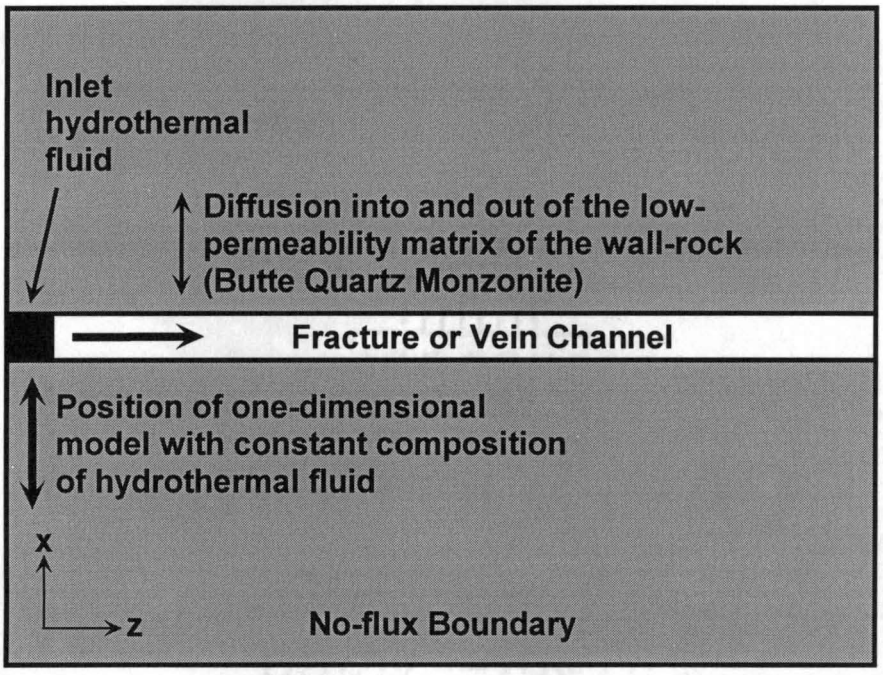

Figure III.3. Schematic representation of the physical model used in the simulations. A discrete fracture is bordered by a low permeability matrix. Advection and dispersion transport solutes in the fracture, but for our purpose concentrations are considered to be constant in the fracture. Diffusion occurs between the fracture and the matrix. The system is isothermal. Fracture and matrix are fluid saturated. The composition of the pore fluid is initially in equilibrium with the host rock. A fluid at the inlet with fixed chemical composition represents the hydrothermal fluid.

Fracture and pore space within the rock matrix are saturated with a single aqueous fluid. The initial pore fluid in the fracture and the matrix is in equilibrium with the host rock (i.e., the Butte Quartz Monzonite). Because the rate of conduction of heat into the rock matrix perpendicular to the fracture is about four orders of magnitude faster than the diffusive transport of the hydrothermal fluid (e.g., Domenico and Schwartz, 1990), it is assumed that once a small volume of fluid has interacted with the rock, the system can be treated under isothermal conditions during the development of the alteration selvages. Fluid flow within the fracture is at steady state. Solute transport occurs within the fracture by advection and dispersion, but for our purposes, concentrations in the fracture are assumed to be constant. Due to the low permeability of the rock matrix, solute transport between fracture and matrix is governed by diffusion only. Constant-concentration (Dirichlet) boundary conditions are employed for the far field deep in the matrix, and it is assumed that fracture spacing is sufficiently large for this to be reasonable. The concentrations of the initial pore fluid are employed as the constant-concentration boundary conditions. In the one-dimensional model presented here, a fixed hydrothermal fluid is assumed at the inlet of the fracture and implements a boundary condition of constant fluid composition in the fracture at all times. This assumption provides and end-member model for the two-dimensional case where fluid advects through the fracture; the constant fluid composition in the fracture

corresponds to water-rock ratios of infinity or to advection rates of more than $1.0x10^5$ times the diffusion rates. In the model, chemical reactions occur within the matrix.

III.5 Governing Equations

III.5.1 Formulation for Multi-Component Diffusion and Reaction

The physics of solute transport in fractured networks are described by two flow continua (e.g., Neretnieks, 1980; Neretnieks and Rasmuson, 1984; Moreno et al., 1985; Moreno et al., 1988). The first continuum is the fracture itself, where advection and dispersion are the governing transport processes. For our purposes, the fracture continuum is considered to have constant chemical concentration. The second continuum is the rock matrix adjacent to the fracture, where diffusion is dominant.

Consider the one-dimensional case where x is the direction perpendicular to a planar fracture. The mass balance equation for diffusive transport and reaction of multiple chemical components in the aqueous fluid and the rock matrix is (e.g., Lichtner, 1991)

$$\frac{\partial}{\partial t}C_i^m = \frac{\partial}{\partial x}\left(D_{px}\frac{\partial C_i^m}{\partial x}\right) - \sum_{a=1}^{N_a} v_{ia} r_a - \sum_{s=1}^{N_s} v_{is} r_s \quad (i = 1,...N_c) \qquad (1)$$

where C_i^m is the concentration of a single aqueous species i of N_c total aqueous species at any location x in matrix m. The pore diffusivity is D_p; the stoichiometric reaction coefficient is v_{ia}; the reaction rate for the formation of an aqueous complex

a is r_a; the stoichiometric reaction coefficient and reaction rate for the formation of a mineral s are v_{is} and r_s, respectively. The sums of the reaction terms $v_{ia}r_a$ and $v_{is}r_s$ are the source-sink terms for aqueous complexation and fluid-mineral interaction, respectively. Note that the (-) sign in the terms $\Sigma v_{ia}r_a$ and $\Sigma v_{is}r_s$ in (1) means that aqueous complexes and minerals, respectively, are formed and the terms act as sinks to the aqueous species.

Changes in the porosity ϕ affect the pore diffusivities D_p due to variations in the restrictivity and tortuosity of the pore space (e.g., Van Barkel and Hertjes, 1974; Ohlsson and Neretnieks, 1995; Cussler, 1996). A best fit through porosity and diffusivity data from low-porosity crystalline rocks from Sweden (Ohlsson and Neretnieks, 1995) gives the following relation which allows the calculation of the feedback between changes in porosity and pore diffusivity due to precipitation or dissolution of minerals (Geiger, 2000)

$$D_p = D_{aq} 1.47 \phi^{0.72} \qquad (2)$$

The aqueous diffusivity D_{aq} of a single solute can be calculated from the Stokes-Einstein relation for the given temperatures and pressures (Cussler, 1996). Since solutes in a multi-component solution interact with each other due to gradients in the chemical and electrical potential, the diffusivity of a single aqueous species is the result of the response of this species to the chemical gradients of all other solutes present (e.g., Lichtner, 1996; Oelkers, 1996). One would need to calculate a matrix of N_c by N_c to calculate the effect of each ionic species on the diffusivities of each other species so as to determine each individual diffusion

coefficient correctly (e.g., Lichtner, 1996; Oelkers, 1996). A simplified approach discussed by Désilets et al. (1997), in which a bulk diffusivity for all aqueous species can be approximated by the harmonic mean of all individual diffusivities, was used in the simulations.

III.5.2 Formulation for Aqueous and Mineral Reactions

The reaction terms in equation (1) are solved by a fully kinetic formulation that has been applied to calculate aqueous and mineral reactions. This allows calculation of reactions within a mixed kinetic-equilibrium system, i.e., accounting for fast reactions near equilibrium and slow reactions far from equilibrium (Steefel and MacQuarrie, 1996). From the principle of detailed balancing (Lasaga, 1984) it follows (Steefel and MacQuarrie, 1996) that an elementary chemical reaction

$$A + B \Leftrightarrow C \tag{3}$$

can be expressed in terms of its forward rate k_f and its backward rate k_b as

$$\frac{d[A]}{dt} = -k_f[A][B] + k_b[C] \tag{4}$$

k_f and k_b balance at equilibrium such that

$$\frac{k_f}{k_b} = \frac{[C]}{[A][B]} = K_{eq} \tag{5}$$

where K_{eq} is the equilibrium constant for each reaction. Individual equilibrium constants are taken from the thermodynamic database Soltherm.HIP (Reed and Palandri, 1999). This results in a system of ordinary differential equations for all

chemical reactions occurring during hydrothermal alteration. Rearranging terms in equations (4) and (5) also gives the rate expression for mineral precipitation and dissolution in terms of the ion activity product Q (Aagaard and Helgeson, 1982; Lasaga, 1984)

$$\frac{d[A]}{dt} = -k_f[A][B]\left(1 - \frac{[C]}{[A][B]}K_{eq}^{-1}\right) = k_f[A][B]\left(1 - QK_{eq}^{-1}\right) \qquad (6)$$

However, since forward rates for mineral precipitation and dissolution are not known at the temperatures of interest at Butte, k_f has been used as a progress variable. The value of the progress variable is determined by the stoichometry of the reaction, i.e., it is 1 if only one mole of the particular species reacts and is e.g., 2 if two moles of the particular species react (Helgeson, 1979). The backward reaction rate, k_b, can then be calculated as $k_b = k_f/K_{eq}$. Since the reaction fronts in the observed mineral assemblages in the sericitic alteration at Butte are sharp and narrow (Reed, 1979), fluid-mineral reactions are transport-limited which implies that the chemical reactions are occurring at a rate that is fast relative to the rate of diffusive transport (c.f., Lichtner, 1991). Speciation calculations are therefore carried out for a long time-step (i.e., until equilibrium).

Precipitation and dissolution of minerals lead to changes in the mass M_s and therefore to modifications of the porosity ϕ. The porosity is directly calculated from the changes in the mineral mass via the conservation of volumes

$$\phi + \sum_{s=1}^{N_s} \frac{M_s}{\rho_s V_{tot}} = 1 \qquad (7)$$

where $\Sigma M_s/(\rho_s V_{tot})$ is the sum of all individual mineral masses M_s over the according density of the minerals ρ_s and the total volume occupied by solids and fluid V_{tot}.

From an analysis of the quasi-stationary state approximation (Lichtner, 1988; 1991), it follows that the initial mineral mass M_s^∞ can be scaled by a factor F less than one to simulate reactive transport efficiently for geologic times (Geiger, 2000). In the results of a reactive transport simulation using scaled mineral masses, time must then be scaled by a factor F^* which is a function of F and the porosity ϕ. This follows from the fact that a smaller mass of a mineral has a faster-moving reaction front than a large mass of the same mineral. The composition of the fluid, however, is independent of the mass of the mineral as long as the mineral is saturated with respect to the fluid (c.f., Reed, 1998). See Lichtner (1988) and Geiger (2000) for a discussion of the details on the properties of scaling the initial mineral mass.

III.5.3 Numerical Solution of the Governing Equations

The computer code CSP3D3.0 (Matthäi and Roberts, 1999) was applied to simulate solute transport and water-rock interactions. CSP3D3.0 solves the transport equations by the finite element method in two dimensions, whereas the system of ordinary differential equations for the chemical reactions is solved with standard solver for ordinary differential equations. Chemical reactions and transport

equations are coupled in CSP3D3.0 via the sequential iterative approach (Yeh and Tripathi, 1989; Yeh and Tripathi, 1991; Zysset et al., 1994). In the sequential iterative approach, the reactive transport equation is alternately solved first for the transport term and then for the reaction term. After every reaction step, a new porosity for the system is calculated from the changes in the mineral volumes after every reaction step, and the pore diffusivity is then updated accordingly and fed into the next transport step.

The finite-element mesh was generated dynamically and is finer close to the fracture (< 0.3 cm grid-spacing) and coarser deep in the matrix (> 0.3 cm grid-spacing). This grants a detailed simulation of the advance of reaction fronts close to the fracture where several reaction fronts form, but also yields a time-efficient simulation by reducing the number of finite elements deep in the matrix where the fluid is largely in equilibrium with the rock and no reaction fronts form. The time-step is 63072.0 seconds, which together with the grid-spacing and the calculated pore diffusivity, D_p, yields a diffusion number N_D less than one and therefore accounts for numerical stability in the simulations (Steefel and MacQuarrie, 1996).

III.6 Modeling Parameters, Initial Conditions, and Chemical Reactions

III.6.1 Mineralogy of the Butte Quartz Monzonite and Pore Fluid Composition

Several assumptions are made in the model to efficiently simulate reactive transport during hydrothermal alteration. First, it is assumed that the system is isothermal (see above), i.e., the rock has the same pressure and temperature as the input hydrothermal fluid. The Butte Quartz Monzonite is initially in equilibrium with a pore fluid at the temperature and pressure for the gray sericitic alteration. We used the water-rock reaction code CHILLER (Reed, 1998) to calculate the mineral assemblage representing the Butte Quartz Monzonite at 400°C and 100 MPa from its oxide composition (Table 1).

Solid solution is not allowed by the calculations. Quartz, microcline, anorthite, albite, annite, tremolite, magnetite, and daphnite comprise a hypothetical stable mineral assemblage making a rock whose composition matches the Butte Quartz Monzonite at 400°C and 100 MPa (Table 2).

Tremolite is the Ca-Mg-amphibole end-member. Annite is the Fe-biotite end-member, and daphnite is the Fe-chlorite. We neglected the oxides TiO_2, P_2O_5, CO_2, BaO, and SO_3 in this process, since their concentrations are small (< 0.6 wt. %) and do not have a significant influence on the alteration process but complicate the numerical solution of the alteration reactions. The calculated mineral assemblage in equilibrium with the pore fluid composition is listed in Table 3. Mineral assemblage and pore fluid compositions comprise the initial condition and

Mineral	Moles[1]	wt %
Quartz	2714.8	20.78
Microcline	608.4	21.57
Anorthite	442.0	15.62
Albite	790.0	26.47
Annite	60.8	3.96
Tremolite	81.4	8.42
Magnetite	90.8	2.68
Daphnite	5.5	0.50

Table III.2. Calculated Mineral Assemblage of the Butte Quartz Monzonite.
[1]Moles of mineral in equilibrium with one kg pore fluid at 400°C and 100 MPa

the far-field Dirichlet boundary condition in the model. The initial mineral mass M_s^{∞} of each mineral has been scaled by a factor F = 1.0×10^{-3}. In the results, time has been scaled by the factor F*(F, ϕ) = 168 while the distance remained unchanged. The following results show the true mineral masses that were back-calculated from the scaled mineral masses used in the numerical simulations.

III.6.2 Hydrothermal Fluid Composition

Although one of the goals of this study is to calculate an approximate composition of the hydrothermal fluid that could have formed the alteration assemblages, a first approximation of its composition is needed as a boundary condition. Since the composition of the hydrothermal fluid at Butte is not known, we used the composition of the fluids estimated for the hydrothermal system of Summitville, Colorado, which approximately represents a fluid of magmatic composition typical for porphyry systems (Getahun, 1994). The composition of the Summitville fluids was recalculated for aqueous species at 400°C and in equilibrium with quartz (Table 3). The fluid is oxidizing, has a pH of 1.3 and a salinity of 2.2 wt. % NaCl.

	Rock	Inlet Fluid	
Species	Pore Fluid[1]	Summitville[2]	Adjusted Fluid[3]
Cl^-	$2.10x10^{-03}$	$2.86x10^{-01}$	$4.38x10^{-01}$
SO_4^{2-}	$2.55x10^{-08}$	$2.86x10^{-01}$	$1.31x10^{-10}$
HCO_3^-	$2.32x10^{-13}$	$1.67x10^{-08}$	$1.73x10^{-08}$
HS^-	$7.48x10^{-06}$	$1.30x10^{-13}$	$2.76x10^{-07}$
$SiO_2(aq)$	$2.78x10^{-02}$	$2.78x10^{-02}$	$2.78x10^{-02}$
Al^{3+}	$3.47x10^{-26}$	$1.57x10^{-06}$	$1.57x10^{-06}$
Ca^{2+}	$7.63x10^{-09}$	$2.84x10^{-05}$	$9.70x10^{-14}$
Mg^{2+}	$4.39x10^{-11}$	$2.83x10^{-07}$	$2.80x10^{-07}$
Fe^{2+}	$1.86x10^{-12}$	$9.70x10^{-06}$	$9.64x10^{-06}$
K^+	$4.78x10^{-04}$	$5.29x10^{-05}$	$5.37x10^{-05}$
Na^+	$2.83x10^{-03}$	$8.52x10^{-05}$	$8.43x10^{-05}$
$AlOH^{2+}$	$2.84x10^{-18}$	$1.38x10^{-07}$	$1.11x10^{-07}$
$AlO_2(OH)(aq)$	$4.27x10^{-06}$	$1.24x10^{-10}$	$7.37x10^{-11}$
AlO_2^-	$3.73x10^{-04}$	$8.16x10^{-14}$	$5.18x10^{-14}$
$CO_2(aq)$	$1.06x10^{-11}$	$1.53x10^{-01}$	$1.53x10^{-01}$
$CaCl^+$	$1.16x10^{-09}$	$5.94x10^{-07}$	$2.42x10^{-16}$
HCl(aq)	$4.33x10^{-09}$	$1.02x10^{-01}$	$1.49x10^{-01}$
$FeCl^+$	$8.10x10^{-13}$	$3.94x10^{-07}$	$4.58x10^{-07}$
KCl(aq)	$3.24x10^{-06}$	$1.04x10^{-06}$	$1.40x10^{-06}$
KOH(aq)	$5.09x10^{-06}$	$6.84x10^{-14}$	$6.31x10^{-14}$
$MgCl^+$	$3.86x10^{-11}$	$2.03x10^{-08}$	$2.34x10^{-08}$
$NaAlO_2(aq)$	$4.77x10^{-04}$	$4.33x10^{-18}$	$2.30x10^{-18}$
NaCl(aq)	$4.35x10^{-05}$	$3.20x10^{-06}$	$4.17x10^{-06}$
NaOH(aq)	$4.07x10^{-05}$	$1.26x10^{-13}$	$1.12x10^{-13}$
OH^-	$5.65x10^{-04}$	$4.21x10^{-09}$	$4.49x10^{-09}$
$H_2S(aq)$	$1.61x10^{-05}$	$4.91x10^{-08}$	$9.97x10^{-02}$
$SO_2(aq)$	$3.29x10^{-11}$	$3.78x10^{-02}$	$6.90x10^{-05}$
HSO_4^-	$3.15x10^{-09}$	$1.16x10^{-01}$	$2.09x10^{-07}$
pH	7.4	1.3	1.3
Salinity[4]	0.01 %	2.20 %	3.32 %

Table III.3. Fluid Composition at 400°C and 100 MPa
[1] Molal concentration. Pore fluid in equilibrium with calculated mineral assemblage of the Butte Quartz Monzonite (Table 2) at 0.5 percent porosity.
[2] Molal concentration. Hydrothermal fluid composition from calculations of the fluids at Summitville, Colorado (Getahun, 1994).
[3] Molal Concentration. Hydrothermal Fluid composition adjusted from oxidizing to reducing to enhance precipitation of pyrite.
[4] Weight percent NaCl (equivalent).

III.6.3 Physical Parameters

The values for the physical input parameters are listed in Table 4. Pressure and temperature for the model were taken for the gray sericitic alteration. Assuming that hydrothermal and pore fluid were dilute, viscosity and density values were extracted from Wagner and Kruse (1998) at 400°C and 100 MPa. The porosity of unaltered, crystalline rocks of granitic composition is commonly around 0.5 percent (Ohlsson and Neretnieks, 1995). The porosity within the fracture (vein channel) is of course 1.0. The initial bulk pore diffusivity was estimated as 5.5×10^{-10} m^2 s^{-1} from the calculated porosity and the harmonic mean of the aqueous diffusivities, which were determined from the Stokes-Einstein relation (Cussler, 1996) for all aqueous species.

Temperature	400°C	Aqueous Diffusivity[1]	1.6×10^{-08} m^2 s^{-1}
Pressure	100 MPa	Pore Diffusivity[1]	5.5×10^{-10} m^2 s^{-1}
Matrix Porosity	0.50 %	Fluid Density[2]	693.0 kg m^{-3}
Fracture Porosity	1.00 %	Fluid Viscosity[2]	8.47×10^{-05} Pa s^{-1}
Rock Density[1]	2712.3 kg m^{-3}	Matrix Depth	1.0 m

Table III.4. Physical Parameters used in the Model
[1] Calculated value
[2] Value from Wagner and Kruse (1998)

III.6.4 Aqueous and Mineral Reactions

Equilibrium constants for the chemical reactions between the aqueous species and the solid minerals in the gray sericitic and sericite with remnant biotite zones were extracted from the thermodynamic database Soltherm.HIP (Reed and Palandri, 1999) at 400°C and 100MPa. All reactions and their associated equilibrium constants are listed in Table 5. Reactions for the aqueous complexes included only species with concentrations higher than $1.0x10^{-10}$ molal. Solid reactions were chosen for the minerals occurring in the calculated mineral assemblage representing the Butte Quartz Monzonite (quartz, anorthite, albite, plagioclase, tremolite, annite, magnetite, daphnite) and furthermore for the alteration products quartz, muscovite, clinozoisite, calcite, anhydrite, and pyrite which are observed in thin sections and core samples of the gray sericitic and sericite with remnant biotite zones.

Reactions for Aqueous Species	log K_{eq}
$H_2O \leftrightarrow OH^- + H^+$	-10.81
$AlOH^{2+} + H^+ \leftrightarrow Al^{3+} + H_2O$	-1.21
$Al^{3+} + 2H_2O(aq) \leftrightarrow AlO_2^- + 4H^+$	-6.44
$HCl \leftrightarrow Cl^- + H^+$	-1.84
$Al^{3+} + 2H_2O \leftrightarrow HAlO_2 + 3H^+$	-0.82
$Al^{3+} + 2H_2O + Na^+ \leftrightarrow NaAlO_2 + 4H^+$	-4.47
$KCl \leftrightarrow Cl^- + K^+$	-0.83
$KOH \leftrightarrow OH^- + K^+$	-1.59
$NaCl \leftrightarrow Cl^- + Na^+$	-1.81
$NaOH \leftrightarrow OH^- + Na^+$	-1.73
$MgCl^+ \leftrightarrow Cl^- + Mg^{2+}$	-3.22
$FeCl^+ \leftrightarrow Cl^- + Fe^{2+}$	-3.08
$CaCl^+ \leftrightarrow Cl^- + Ca^{2+}$	-2.45
$CO_2 + H_2O \leftrightarrow HCO_3^- + H^+$	-9.22
$H_2S \leftrightarrow HS^- + H^+$	-7.89
$HSO_4^- \leftrightarrow SO_4^{2-} + H^+$	-6.92
$SO_2 + H_2O = 1.75H^+ + 0.75\ SO_4^{2-} + 0.25HS^-$	-9.92
Reactions between Minerals and Aqueous Species[1]	
Quartz $\leftrightarrow SiO_2(aq)$	-1.56
Microcline $+ 4H^+ \leftrightarrow K^+ + Al^{3+} + 3SiO_2(aq) + 2H_2O(aq)$	-5.31
Albite $+ 4H^+ \leftrightarrow Na^+ + Al^{3+} + 3SiO_2(aq) + 2H_2O(aq)$	-4.53
Anorthite $+ 8H^+ \leftrightarrow Ca^{2+} + 2Al^{3+} + 2SiO_2(aq) + 4H_2O(aq)$	-6.12
Annite $+ 10H^+ \leftrightarrow K^+ + 3Fe^{2+} + 3SiO_2(aq) + 6H_2O(aq)$	2.13
Tremolite $+ 14H^+ \leftrightarrow 2Ca^{2+} + 5Mg^{2+} + 8SiO_2(aq) + 8H_2O(aq)$	18.95
Magnetite $+ SO_2(aq) + 4H^+ \leftrightarrow 3Fe^{2+} + 2H_2O(aq) + SO_4^{2-}$	-5.06
Daphnite $+ 16H^+ \leftrightarrow 5Fe^{2+} + 2Al^{3+} + 3SiO_2(aq) + 12H_2O(aq)$	-1.39
Muscovite $+ 10H^+ \leftrightarrow K^+ + 3Al^{3+} + 3SiO_2(aq) + 6H_2O(aq)$	-14.02
Clinozoisite $+ 13H^+ \leftrightarrow 2Ca^{2+} + 3Al^{3+} + 3SiO_2(aq) + 7H_2O(aq)$	-6.09
Calcite $+ H^+ \leftrightarrow Ca^{2+} + HCO_3^-$	-2.60
Anhydrite $+ H^+ \leftrightarrow Ca^{2+} + HSO_4^-$	-3.73
Pyrite $+ H_2O(aq) \leftrightarrow Fe^{2+} + 1.75HS^- + 0.25H^+ + 0.25\ SO_4^{2-}$	-18.76

Table III.5. Reactions and Equilibrium Constants used in the Calculations. Data from Soltherm.HIP (Reed and Palandri, 1999) at 400°C and 100 MPa.
[1] Species with charges are aqueous species.

III.7 Results with the Summitville Fluid

III.7.1 Mineral Mass Profiles

Graphs that depict cross sections of the calculated mineral assemblages after 25 years through the diffusion halo perpendicular to the fracture are shown in Figure 4. The simulations with the Summitville fluid composition show a successive dissolution of the minerals composing the Butte Quartz Monzonite. In other words, the locations of the reaction fronts are different for each mineral. Albite and microcline were completely dissolved along the fracture and their dissolution fronts have advanced about 2.0 cm into the rock matrix (Fig. 4a). Albite dissolved at a slightly higher rate than microcline, since the initial mass of albite was higher than the initial mass of microcline. Smaller amounts of albite were re-precipitated close to the fracture near the location where H^+ was being consumed by the dissolution of anorthite. Apparently, Na^+ produced by the dissolution of albite diffused down a concentration gradient into the fracture, and where the activities of Al^{3+} and $SiO_2(aq)$ were high due to the dissolution of anorthite, the solubility of albite was exceeded so that albite precipitated. Muscovite almost entirely replaces microcline along the fracture (Fig. 4b). Anorthite was surprisingly more stable than the potassium and sodium feldspar end-members, and after 25 years about 15 moles of its initial mineral mass were still present close to the fracture (Fig. 4a). The reaction front of tremolite has advanced about 0.7 cm into the matrix (Fig. 4a). The dissolution of tremolite is a function of the activity ratio of

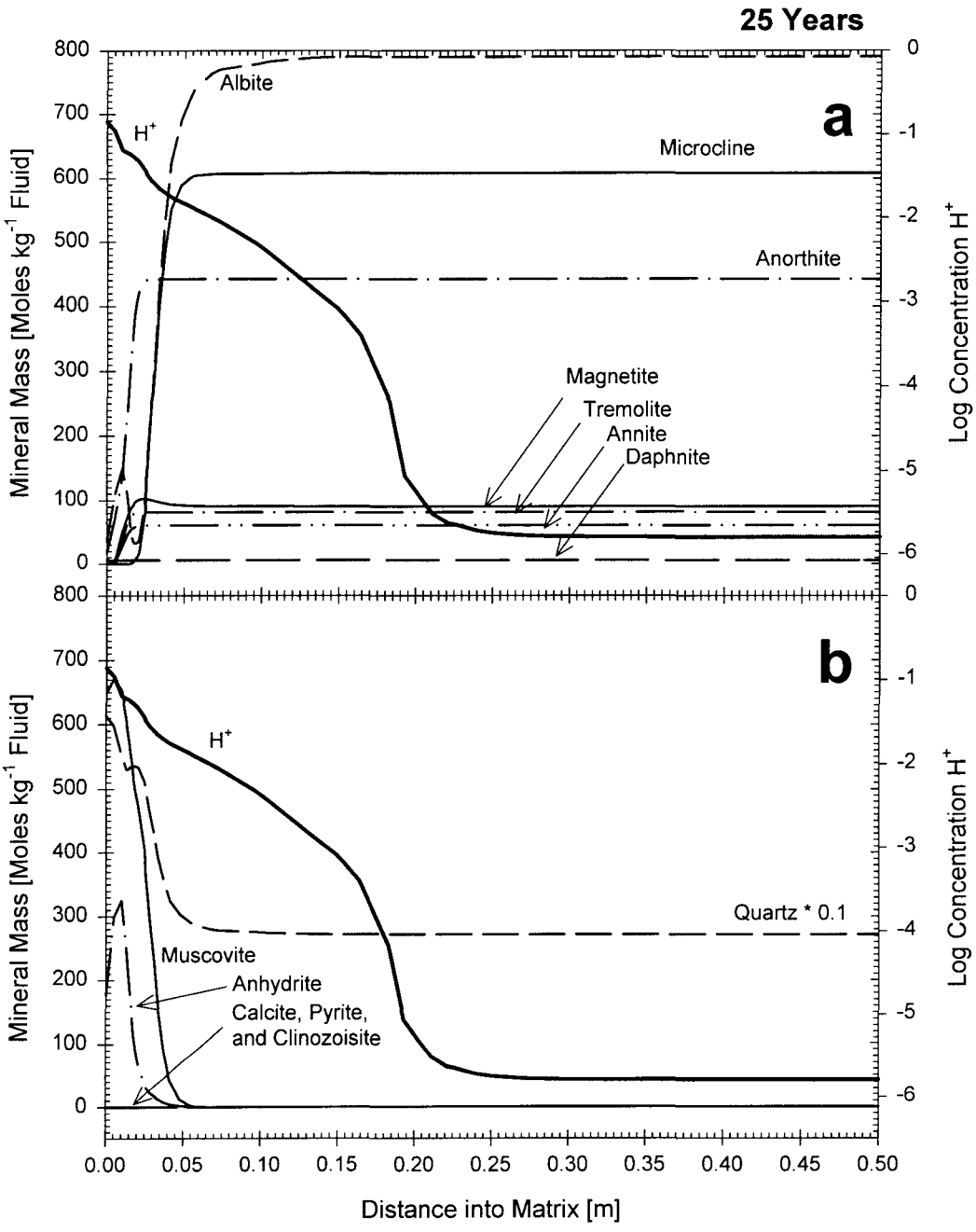

Figure III.4. Masses of the primary (a) and secondary minerals (b) after 25 years. The plots show cross sections perpendicular to the fracture through the mineral assemblages. The Summitville Fluid composition (Table 3) was used as the input for the hydrothermal fluid. Note that the mass of quartz is scaled in the plot by a factor 0.1.

$Ca^{2+}/(H^+)^2$ and is stable where this ratio is high. Therefore, where dissolution of anorthite takes place and raises the $Ca^{2+}/(H^+)^2$ ratio, tremolite is stabilized. The anorthite dissolution front therefore corresponds closely with the tremolite reaction front (Fig. 4a). Anorthite was completely dissolved along the fracture after about 30 years. The calcium set free by the dissolution of anorthite and tremolite was precipitated as anhydrite, but no clinozoisite or calcite were precipitated (Fig. 4b). The Fe-biotite annite was also completely dissolved along the fracture. However, the annite reaction front trailed all other mineral dissolution fronts and is closest to the fracture (Fig. 4a). Its reaction front advanced about 0.6 cm into the matrix, and the edge of the annite front is the mineralogic transition that marks the boundary from the gray sericitic zone to the sericite with remnant biotite zone in natural samples from Butte (Fig. 2). The dissolution of microcline and magnetite caused the activity ratios of K^+/H^+ and the $Fe^{2+}/(H^+)^2$, respectively, to increase, which stabilizes annite. The silica set free by the dissolution of feldspars, biotite, and amphibole directly precipitated as quartz (Fig. 4a). The mass of quartz decreased with increasing distance into the matrix. The Fe-chlorite daphnite was entirely stable under the present conditions and was not dissolved (Fig. 4a). Magnetite dissolved along the fracture and its reaction front advanced about 0.7 cm deep into the matrix (Fig. 4a). However, the free Fe^{2+}(aq) released by magnetite dissolution did not precipitate as pyrite (Fig. 4b) since the hydrothermal fluid was oxidizing and lacked sulfide (H_2S, HS^-) for the pyrite precipitation. Approximately 10 moles

of magnetite were re-precipitated about 1.5 cm into the matrix at a position just outside the annite dissolution front.

The concentration profile of the hydrogen ion shows a decrease in concentration from the fracture into the matrix. The hydrogen ion concentration is very sensitive to the mineral assemblage at different locations in the rock, and kinks in the slope of the concentration profile are related to the successive edges of mineral reaction fronts (Fig. 4a).

The mineral reaction fronts observed in samples of the gray sericitic and sericite with remnant biotite alteration are always sharp and narrow (Reed, 1979). This observation leads to the assumption that the mineral-fluid reactions are transport-limited rather than surface-limited (Lichtner, 1991). All simulated reaction fronts, however, display widths that are broader than expected, i.e., the mineral masses increase gradually into the matrix in the case of a dissolution front and decrease in the case of a precipitation front (Fig. 4). This "stretching" of a mineral reaction front is caused by the decoupling of the reaction step and transport step in the sequential iterative method. Decoupling of the reaction and transport step allows diffusion of aqueous species in the rock matrix before the first reaction step. The fluid is therefore at different stages of disequilibrium with the host rock, yielding different amounts of dissolved and precipitated minerals. An infinitely small time-step would yield sharp reaction zones with zero thickness (Geiger, 2000). Increasing the calculation time allowed for every reaction step within the

ordinary differential equation solver to a very large time, i.e., finding the equilibrium solution for every reaction step also increases the sharpness of the reaction fronts slightly.

III.7.2 Comparison of the Simulated and the Observed Mineral Assemblages

The simulations using the composition of the Summitville fluids (Getahun, 1994) as the input for the hydrothermal fluid display the general trend of the evolution of the hydrothermal alteration zones after 25 years (Fig. 4a and 4b). Minerals dissolve and precipitate at different locations, which leads to individual reaction fronts for each mineral. Those reaction fronts advance at different rates and therefore form a distinct succession of minerals. Most significant here is the fact that the annite dissolution front trails all other dissolution fronts (with the exception of the anorthite front), and marks the transition from the gray sericite to the sericite with remnant biotite zone.

Although the simulations with the Summitville fluids show the general pattern of the development of the alteration sequences, there are differences between the simulated minerals and the actual minerals observed in the alteration envelopes. Anorthite seems to dissolve too slowly in comparison to the other feldspars, while the re-precipitation of albite has not been observed in the gray sericite alteration. The plagioclase dissolution front, i.e., the albite and anorthite fronts, should have advanced farthest into the matrix, because the occurrence of

fresh plagioclase along a fracture in drill cores commonly marks the edge of unaltered Butte Quartz Monzonite in the sericitic pre-Main State alteration (Fig. 2). Pyrite does not precipitate at all in the simulations although it is the most significant disseminated sulfide of the sericitic pre-Main Stage alteration. Further, calcite and clinozoisite also do not precipitate although they sometimes can be found in small quantities in the gray sericitic alteration.

III.8 Results with a Reducing Hydrothermal Fluid

III.8.1 Adjustment of Summitville Fluid to Improve Simulations

The deviation of the simulated mineral profiles (Fig. 4) from the observed mineral profiles (Fig. 2) of the sericitic pre-Main Stage alteration is most likely caused by the use of the Summitville hydrothermal fluid whose composition in some ways does not resemble the reacting fluid that has caused the gray sericitic and sericite with remnant biotite alteration zones. A key assumption in the model is that all reactions are transport-limited. This implies that small changes in the chemical concentration gradients between the hydrothermal and pore fluid can have a significant influence on the evolution of the reaction fronts, as solutes are transported to and from the reaction fronts at different rates. It therefore should be possible to modify the Summitville hydrothermal fluid composition until a series of mineral assemblages are produced that resemble the observed mineral profiles. Therefore, we adjusted the Summitville fluid composition for a second simulation

from oxidizing to reducing (i.e., by increasing sulfide to sulfate ratio at constant total sulfur) to enhance the precipitation of pyrite and decrease the precipitation of anhydrite so as to correspond to high pyrite/anhydrite ratios in natural samples. Furthermore, we decreased the Ca^{2+} concentration in the hydrothermal fluid so as to promote the dissolution of tremolite and anorthite, which are not found close to the fracture in natural samples.

III.8.2 Mineral Mass Profiles

Mineral concentration profiles at 25 years for a simulation that uses a reducing hydrothermal fluid with a lower calcium concentration but unchanged pH (Table 3) as the input conditions are shown in Figure 5. Note that the salinity of the reducing hydrothermal fluid increased to 3.32 % NaCl, because the charge balance of the solution was adjusted via the concentration of Cl^-.

Changing the hydrothermal fluid from oxidizing to reducing has little impact on the dissolution of minerals in the Butte Quartz Monzonite, i.e., the pattern of successive reaction fronts remains approximately the same. Some of the dissolution reactions occur at a lower rate (i.e., hydrolysis of annite, anorthite, and tremolite), whereas others occur at a higher rate (i.e., hydrolysis of albite, magnetite, and microcline) in comparison to the oxidizing hydrothermal fluid (c.f., Fig. 4 and 5).

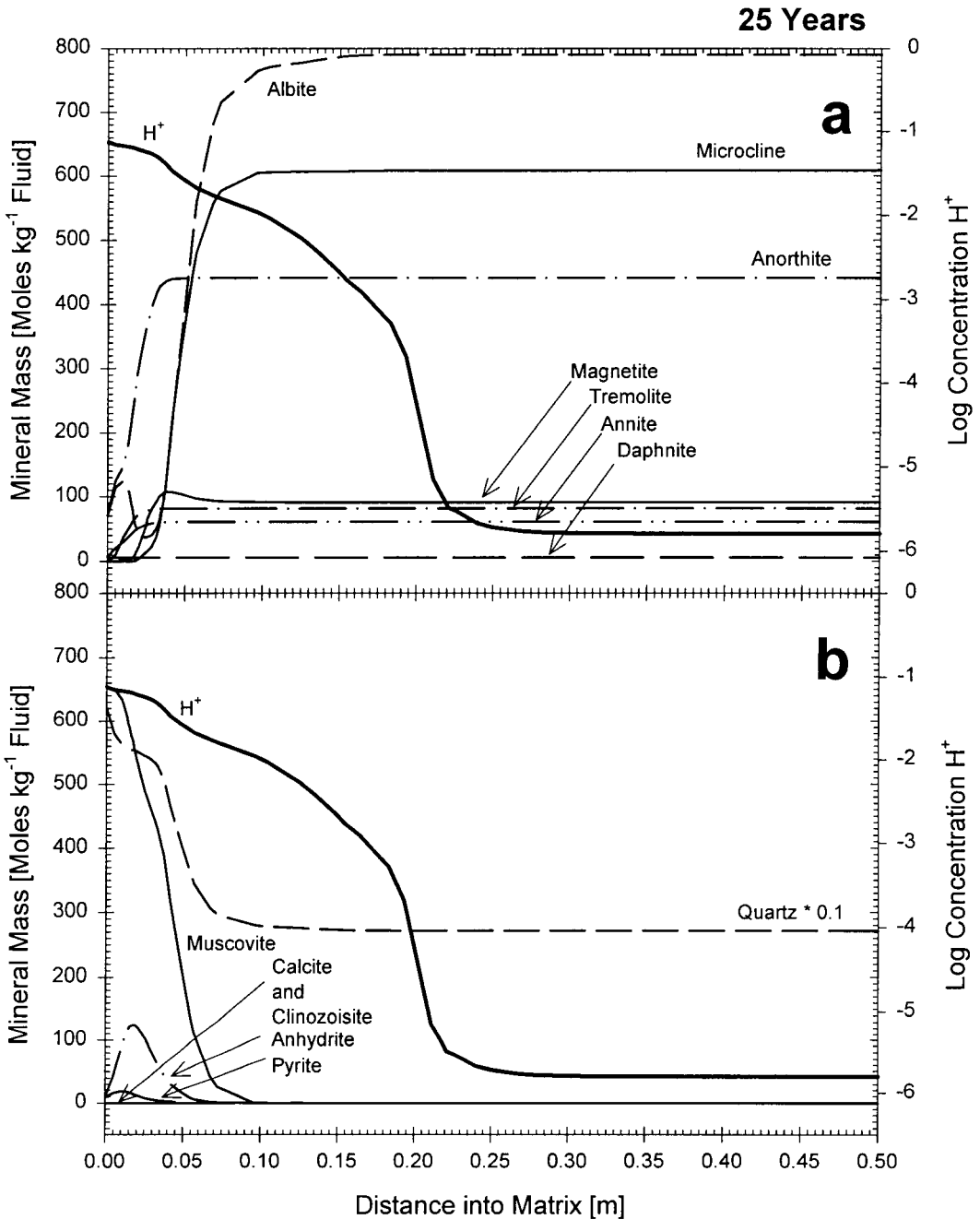

Figure III.5. Masses of the primary (a) and secondary minerals (b) after 25 years. The plots show cross sections perpendicular to the fracture through the mineral assemblages. A reducing hydrothermal with lower Ca^{2+} concentration (Table 3) was used as the input for the hydrothermal fluid. Note that the mass of quartz is scaled in the plot by a factor 0.1.

The most significant difference caused by the change of the hydrothermal fluid from oxidizing to reducing is that pyrite precipitated and anhydrite precipitation decreased. Up to 10 moles of pyrite precipitated over the same interval in which magnetite dissolved. The reduced precipitation of anhydrite also decreased the dissolution rates of tremolite and anorthite, because the Ca^{2+} concentration in the fluid remained higher and stabilized anorthite and tremolite slightly more than under oxidizing conditions. The dissolution fronts of albite and microcline advanced faster in comparison to the oxidizing fluid to a total distance of 2.5 cm into the matrix. About eighty percent of anorthite was dissolved along the fracture. Tremolite is completely dissolved along the fracture after 25 years (Fig. 5a). The dissolution of annite also occurred at a lower rate under reducing conditions. With the exception of daphnite, which appeared to be entirely stable, annite is still the mineral that reacted at the lowest rate and was present closest to the fracture. There was still about10 percent of the initial mass of annite present along the fracture so that an inner gray sericitic envelope without biotite is not simulated after 25 years (Fig. 5a). Magnetite dissolved faster under reducing conditions, because Fe^{2+}(aq) precipitation of pyrite reduced the Fe^{2+}(aq) concentration of the fluid, which acts to destabilize magnetite. The magnetite dissolution front advanced about 2.0 cm into the matrix. Owing to the formation of pyrite, the amount of re-precipitated magnetite decreased (Fig. 5a) in comparison to the oxidizing fluid (Fig. 4a).

III.8.3 Changes in Porosity and Diffusivity

The feedback between mineral reactions and solute transport is of key interest during reactive transport. Precipitation and dissolution of minerals will change the porosity of the wall-rock, which may lead to gradients in the pore diffusivity if the porosity changes are large enough. Simulations using the Summitville fluid adjusted to reducing conditions yield a small porosity gradient perpendicular to the fracture (Fig. 6). The simulated hydrothermal alteration of the Butte Quartz Monzonite causes only a slight increase in porosity during sericitic alteration. The precipitation of quartz and muscovite counterbalance the dissolution of feldspar and other minerals and keeps the porosity from changing very much. After 30 years, the porosity increased from its initial value of 0.50 to 0.60 percent (note that the values are rounded to the first digit). Since diffusivities change the porosity to the 0.72 power (Equation 2), the diffusivity increases from its initial value of 5.54×10^{-10} m^2 s^{-1} to 6.09×10^{-10} m^2 s^{-1}.

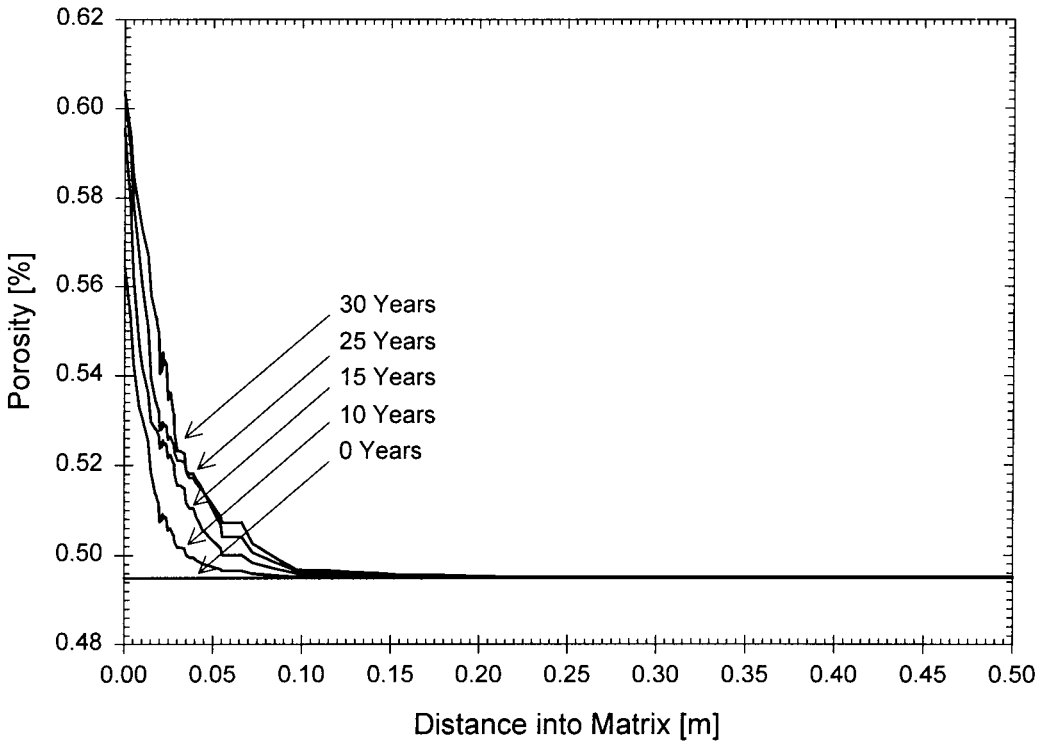

Figure III.6. Temporal development of the porosity perpendicular to the fracture due to hydrothermal alteration. The porosity increases only slightly from its original value of 0.50 % to 0.60 % after 30 years. Note that the values are rounded to the first digit in the text. Porosity increases slightly, despite precipitation of new alteration minerals, because original rock minerals are removed in slightly greater volumetric amounts. Since diffusivity changes only to the 0.72 power of porosity, the diffusivities change little (less than 10 %) and solute transport is not significantly affected by hydrothermal alteration. Note that the oscillations in the porosity values are due to a minor numerical error. Porosities are calculated for every node and mineral assemblages change slightly from node to node. A three-point moving average was used to smooth the largest oscillations in this plot.

III.9 Discussion

III.9.1 General Features

The simulations using a reducing version of the Summitville fluid composition form a succession of mineral reaction fronts that are similar to the observed zonation from inner gray sericitic to outer sericite with remnant biotite alteration zones (Fig. 5). The fluid, thus, is a first order approach to the actual composition of the Butte hydrothermal fluid. The fluid was highly acidic, reducing, sulfide-rich, and low salinity, which appears to be in good agreement with the limited fluid inclusion data available for the sericitic alteration zone. It should be clearly stated that this simulated fluid composition is not entirely representative of the Butte hydrothermal fluid and rather yields a crude idea of the general properties of the hydrothermal fluid. Distinct values for the concentration of each individual species are almost impossible to calculate, since activity coefficients of the aqueous species are not well known at 400°C, and relatively small changes in the chemical concentration of aqueous species may have significant impacts on the types of chemical reactions and their positions.

The simulated hydrothermal alteration assemblages are characterized by a sequence of mineral reaction fronts. The location of each individual reaction front is dependent on two factors. First, the increase in pH of the fluid with distance into the matrix forms a distinct pattern of mineral dissolution and precipitation fronts because hydrolysis fluid-mineral reactions are pH-sensitive. Secondly, hydrolysis

of minerals also produces increased concentrations of other aqueous species and imposes concentration gradients of these species on the solution. The movement of mineral reaction fronts is therefore not only pH-dependent, but driven by the concentrations of other species (Lichtner, 1988; 1991).

III.9.2 Comparison with Natural Zoned Envelopes at Butte

Within the simulated reaction pattern (Fig. 5), microcline is the mineral reacting at the highest rate. This is problematic because the occurrence of plagioclase marks the edge of fresh Butte Quartz Monzonite. The problem of the slow dissolution of anorthite and albite relative to microcline might be owing to the lack of inclusion of solid solution in the simulations. Simulations are carried out for feldspar, biotite, and amphibole end-members, which could disturb the dissolution and precipitation pattern. The lack of solid solution most notably has an impact on the dissolution of plagioclase, which occurs in the Butte Quartz Monzonite as a solution of albite and anorthite rather than the two individual end-members. The actual rate of plagioclase dissolution is therefore a combination of the simulated albite and anorthite dissolution reaction rates (C.I. Steefel, pers. comm., 1999). Solid solutions of minerals, however, are always thermodynamically more stable than a mixture of their end-members. The true plagioclase dissolution front would therefore trail the modeled microcline front. Increasing the pH and further decreasing the Ca^{2+} activity of the hydrothermal fluid barely enhances the

dissolution of anorthite. This suggests that the thermodynamic data for the dissolution reaction of anorthite might be inaccurate. A faster dissolution of anorthite would yield faster dissolution of plagioclase as a solid solution relative to microcline.

The dissolution of feldspars causes precipitation of muscovite, quartz, and anhydrite. The reaction rates of those alteration products are strongly coupled to the dissolution of microcline, albite, and anorthite. The hydrolysis of tremolite occurs at a lower rate. The dissolution of anorthite fixes the Ca^{2+} to H^{+} activity ratio in the fluid and stabilizes tremolite (Fig. 5). Calcium, however, does not precipitate as calcite or clinozoisite, despite the fact that these alteration products have been observed as trace to minor minerals in the sericitic pre-Main stage assemblages. It should be noted that anhydrite may have been partly dissolved by the later an lower temperature Main Stage fluids. Therefore, consistent with the retrograde solubility of anhydrite below temperatures of 375°C (Blount and Dickson, 1968), anhydrite concentration may be artificially low in the observed alteration assemblage at Butte in comparison to the simulated assemblage.

Magnetite dissolution is closely related to the precipitation of pyrite under reducing conditions because it supplies Fe^{2+}(aq). Additionally, the Fe^{2+}(aq) released by the dissolution of magnetite tends to stabilize the Fe-biotite annite. The dissolution of annite is also reduced by the addition of K^{+} to the fluid via the dissolution of microcline. Hence, the annite reaction front trails all other dissolution fronts and marks the transition from the gray sericitic to the sericite with remnant

biotite zone (Fig. 5). The simulations therefore predict the observed alteration assemblages of the sericitic pre-Main Stage alteration, where muscovite, quartz, and pyrite (± anhydrite) can be found closest to the fracture. Since the annite dissolution front trails all other reaction fronts, biotite is the first mineral of the Butte Quartz Monzonite that can be found in the matrix. Muscovite, quartz, and pyrite, however, completely replace all feldspars and amphiboles in the inner selvage where biotite is remnant consistent with both natural observations and simulations (Fig. 2).

Simulations imply that the pattern of reaction fronts is fully established after approximately 30 years when the annite dissolution front starts to advance from the fracture into the matrix and the gray sericitic alteration zone is completely developed. The simulated time necessary to fully develop the sericitic pre-Main Stage alteration can vary for three reasons (Geiger, 2000). Two reasons are related to numerical approximations in the simulations due to the decoupling of the reaction and transport step in the sequential iterative method. First, the time-stepping chosen in the simulations influences the time necessary to dissolve a mineral. Secondly, mineral mass scaling influences the time to dissolve a mineral. Finally, the initial composition of the hydrothermal fluid, which is fixed in the simulations, can influence the time frame for the development of the sericitic pre-Main Stage alteration. The composition of the hydrothermal fluid, most notably the pH, has a strong impact on the time necessary to develop the full sericitic pre-Main Stage alteration since mineral-reactions are transport controlled. However, those

variations are not related to numerical errors and rather follow from the fact that the composition of the hydrothermal fluid is only estimated and cannot be calculated exactly. The time necessary to fully develop the sericitic pre-Main Stage alteration therefore cannot be predicted exactly, but was probably less than hundred years. This is in good agreement with the time frame Steefel and Lichtner (1994; 1998) calculated for the diffusion-controlled chemical alteration along a fracture of highly reactive low-temperature systems. If the simulations could be fully carried out under local equilibrium conditions and with very small time-stepping and grid spacing, the reaction fronts would be much sharper than depicted (Geiger, 2000).

The theoretical models of Lichtner (1988, 1991), and Lichtner and Balashov (1993) have shown that the locations of the mineral reaction fronts must remain constant relative to each other, once the reaction pattern has been established. Natural examples of zoned mineral selvages, such as Butte, contain numerous examples of concentrically zoned mineral assemblages that yield the same conclusion. Despite widths of selvages that vary by a factor of 10, reflecting very different elapsed times of alteration, the concentric zonation sequence is always the same and is in the same order. Since the locations of mineral reaction fronts move as the square root of time if diffusion is the governing solute transport process, the sequence of the reaction pattern is time-independent and the reaction fronts will only advance deeper into the matrix with time while maintaining concentration positions relative to each other (Lichtner, 1991). The relative widths of the reaction zones therefore remain constant. The annite dissolution front will therefore always

trail all other mineral reaction fronts and constantly mark the transition from the gray sericitic to sericite with remnant biotite zone. Once annite is completely dissolved along the fracture (> 25 years), the gray sericitic alteration zone is fully established. Since the feldspar dissolution front that marks the edge of the fresh Butte Quartz Monzonite and the annite dissolution front both advance as the square root of time, the widths of the gray sericitic and sericite with remnant biotite zones increase at a constant rate relative to each other. The ratio of those two widths therefore remains constant.

From the physical properties of reactive transport in a discrete fracture, it follows that alteration envelopes are wedged along a fracture because diffusion of reactive solutes in the matrix is slower than advection of reactive solutes in the fracture (Steefel and Lichtner, 1998a). It therefore follows that the thickness of the alteration zones along a fracture decreases with increasing distance away from the hydrothermal fluid source, which eventually can lead to the pinching out of the alteration zones.

Hydrothermal alteration of the Butte Quartz Monzonite has only minor affects on the porosity of the wall-rock because the porosity increases only from 0.5 to 0.6 percent (Fig. 6). Three important facts deduce from this increase in porosity. First, there is always enough pore space to precipitate alteration minerals, since the porosity increases with time. Secondly, since the change in porosity is small and the diffusivity changes only as porosity to the power of 0.72, the gradient in the diffusivity perpendicular to the fracture is small and transport is virtually

unaffected. Thirdly, since the porosity increases only to 0.6 percent adjacent to the fracture, the permeability of the rock matrix remains very low and no significant fluid flow occurs within the matrix.

III.10 Conclusions

Using the vein geology, geochemical modeling, and reactive transport simulations, we were able to successfully model the development of the sericitic pre-Main Stage alteration sequences at Butte, Montana. Five conclusions come from this study.

First, a reducing, low salinity hydrothermal fluid with low pH can produce the observed gray sericitic and sericite with remnant biotite alteration envelopes. Reactions between the hydrothermal fluid and the rock matrix cause the dissolution of feldspars, biotite, and amphibole, which are replaced by quartz, muscovite, pyrite ± anhydrite. The time span necessary to completely evolve the hydrothermal alteration assemblage was probably less than one hundred years.

Secondly, the evolution of the alteration sequences is characterized by a succession of individual mineral reaction fronts. The different dissolution and precipitation fronts advance at different rates and form a distinct pattern of minerals, which is purely driven by the diffusion and concentration gradients of the individual aqueous species as predicted by chemical thermodynamics and diffusion theory. The first mineral to react is microcline at the outer edge of the alteration

zone against fresh Butte Quartz Monzonite. Plagioclase dissolves too slowly in our simulation, which could be due to incorrect thermodynamic data for the hydrolysis of anorthite. The annite dissolution front trails all other reaction fronts and marks the transition from the gray sericitic to the sericite with remnant biotite alteration zone. An inner gray sericitic and an outer sericite with remnant biotite zone is therefore present at all times once the annite dissolution front starts to advance into the matrix.

Thirdly, from the physical properties of reactive transport in a discrete fracture, it follows that alteration envelopes along a fracture are wedged because diffusion of reactive solutes in the rock matrix occurs at a lower rate than advection in the fracture (Steefel and Lichtner, 1998a). This can cause a decrease in the widths and wedging of the alteration zones along the fracture.

Fourthly, hydrothermal alteration has little effect on the porosity of the Butte Quartz Monzonite, and the solute transport behavior is therefore not influenced by significant changes in the diffusivity or permeability.

Lastly, since the sericitic pre-Main Stage alteration is common for many other porphyry copper deposits around the world, this study also yields insight about the development of a very common type of hydrothermal alteration.

III.11 Acknowledgements

We are greatly indebted to Carl Steefel of the Lawrence Livermore National Laboratory for his interest, help, and fruitful discussions during the course of this work. The first author would also like to thank the Radiation Center at Oregon State University, especially Erwin Schütfort and Steve Binney, for the financial support throughout this Masters thesis. Financial support for the geologic studies at Butte was supported by the National Science Foundation, grant NSF-EAR-9614683.

III.12 References

Aagaard, P. and Helgeson, H.C., 1982, Thermodynamic and kinetic constrains in reaction rates among minerals and aqueous solutions, I. Theoretical considerations. American Journal of Science, v. 282, 237-285.

Beaudoin, G. and Therrien, R., 1999, Sources and drains; major controls of hydrothermal fluid flow in the Kokanee Range, British Columbia, Canada. Geology, v.27, 883-886.

Blount, C.W. and Dickson, F.W., 1968, The solubility of anhydrite ($CaSO_4$) in NaCl-H_2O from 100 to 450 degrees C and 1 to 1000 bars. Geochimica et Cosmochimica Acta, v. 33, 227-245.

Brimhall, G.H., 1977, Early fracture controlled disseminated mineralization at Butte, Montana. Economic Geology, v. 72, 37-59.

Brimhall, G.H., 1979, Lithologic determination of mass transfer mechanisms of multiple-stage porphyry copper mineralization at Butte, MT: Vein formation by hypogene leaching and enrichment of potassium-silicate. Economic Geology v. 74, 556-590.

Brimhall, G.H., 1980, Deep hypogene oxidation of porphyry copper potassium-silicate protore at Butte, Montana: A theoretical evaluation of the copper remobilization hypothesis. Economic Geology, v. 75, 348-409.

Brimhall, G.H. and Ghiorso, M.S., 1983, Origin and ore-forming consequences of the advanced argillic alteration process in hypogene environments by magmatic gas contamination of meteoric fluids. Economic Geology, v. 78, 73-90.

Brown, J.G., Bassett, R.L., and Glynn, P.D., 1998, Analysis and simulation of reactive transport of metal contaminants in ground water in Pinal Creek, Arizona. Journal of Hydrology, v. 209, 225-250.

Cathles, L.M., 1983, An analysis of the hydrothermal system responsible for deposition of massive sulfide deposition in the Hokuroku Basin of Japan. Economic Geology Monograph 5, 439-487.

Cussler, E.L., 1996, Diffusion: Mass transfer in fluid Systems. Cambridge University Press, 525 pages.

Désilets, M., Proulx, P., and Soucy, G., 1997, Modeling of multicomponent diffusion in high temperature flows. International Journal Heat Mass Transfer, v. 40, 4273-4278.

Dilles, J.H. and Einaudi, M.T., 1992, Wall-rock alteration and hydrothermal flow paths about the Ann-Mason porphyry copper deposit, Nevada--A 6 km vertical reconstruction. Economic Geology, v. 87, 1963-2001.

Domenico, P.A. and Schwarz, F.W., 1990, Physical and Chemical Hydrogeology. John Wiley and Sons, 824 pages.

Engesgaard, P. and Kipp, K.L., 1992, A geochemical model for redox-controlled movement of mineral fronts in groundwater-flow systems: A case of nitrate removal by oxidation of pyrite. Water Resources Research, v. 28, 2829-2843.

Geiger, S., 2000, Reactive transport modeling in discrete fractures: Applications to the formation of sericitic hydrothermal alteration at Butte, Montana. MS Thesis, Dept. of Geosciences, Oregon State University, 124 pages.

Getahun, A., 1994, Fluid-rock reaction and mineralization in two high-level volcanic settings: Augustine Fumaroles and the Summitville acid-sulfate copper-gold deposit. Ph.D. dissertation, University of Oregon, 331pages.

Glynn, P.D. and Brown, J.G., 1996, Reactive transport modeling of acidic metal-contaminated groundwater at a site with sparse spatial information. In: Lichtner, P.C., Steefel, C.I., and Oelkers, E.H. (eds.), Reactive Transport in Porous Media. Reviews in Mineralogy, v. 34, 377-438.

Gustafson, L.N. and Hunt, J.P., 1975, The porphyry copper deposits at El Salvador, Chile. Economic Geology, v.70, 857-912.

He, W., Zhengyu, B., and Tieping, L., 1999, One-dimensional reactive transport models of alteration in the Tongchang porphyry copper deposit, Dexing District, Jiangxi Province, China. Economic Geology, v. 94, 307-323.

Helgeson, H.C., 1979, Mass transfer among minerals and hydrothermal solutions. In: Barnes, H.L. (ed.), Geochemistry of hydrothermal ore deposits, 2nd edition, 421-469. John Wiley & Sons.

Houston, R.A., 1999, The Butte District, Montana - New field data and reassessment of post-mineral structural tilting. Geological Society of America, Annual Meeting 1999, Denver, Abstract with Programs, v. 31, p. A-382.

Johnson, J.W., Knauss, K.G., Glassley, W.E., DeLoach, L.D., and Tompson, A.F.B., 1998, Reactive transport modeling of plug-flow reactor experiments: quartz and tuff dissolution at 240°C. Journal of Hydrology, v. 209, 81-111.

Klepper, M.R., 1973, Geology of the Southern Part of the Boulder Batholith. Guide Book for the Butte Field Meeting of the Society of Economic Geologists 1973, p. B 1-5.

Knopf, A., 1957, The Boulder Batholith of Montana. American Journal of Science, v. 255, 81-103.

Lasaga, A.C., 1984, Chemical kinetics of water-rock interactions. Journal Geophysical Research, v. 89, 4009-4025.

Lasaga, A.C. and Rye, D.M., 1993, Fluid flow and chemical reaction kinetics in metamorphic systems. American Journal of Science, v. 293, 2169-2175.

Lichtner, P.C., 1985, Continuum model for simultaneous chemical reactions and mass transport in hydrothermal systems. Geochimica et Cosmochimica Acta, v. 49, 779-800.

Lichtner, P.C., Oelkers, E. H., and Helgeson, H.C., 1986, Interdiffusion with multiple precipitation / dissolution reactions: Transient model and steady-state limit. Geochimica et Cosmochimica Acta, v. 50, 1951-1966.

Lichtner, P.C., 1988, The quasi-stationary state approximation to coupled mass transport and fluid-rock interaction in a porous medium. Geochimica et Cosmochimica Acta, v. 52, 143-165.

Lichtner, P.C., 1991, The quasi-stationary state approximation to fluid/rock interaction: local equilibrium revisited. In: Ganguly, J. (ed.) Diffusion, atomic ordering and mass transport. Advances in Physical Geochemistry, v. 8, 454-562. Springer Verlag.

Lichtner, P.C., 1992, Time-space continuum description of fluid / rock interaction. Water Resources Research, v. 28, 3135-3155.

Lichtner, P.C. and Biino G.G., 1992, A first principles approach to supergene enrichment of porphyry copper protore. I. Cu-Fe-S-H_2O subsystem. Geochimica et Cosmochimica Acta, v. 56, 3987-4013.

Lichtner, P.C., 1993, Scaling properties of time-space kinetic mass transport equations and the local equilibrium limit. American Journal of Science, v. 293, 257-296.

Lichtner, P.C. and Balashov, V.N., 1993, Metasomatic zoning: appearance of ghost zones in the limit of pure advective mass transport. Geochimica et Cosmochimica Acta, v. 57, 369-387.

Lichtner, P.C., 1996, Continuum formulation of multicomponent-multiphase reactive transport. In: Lichtner, P.C., Steefel, C.I., and Oelkers, E.H. (eds.), Reactive Transport in Porous Media. Reviews in Mineralogy, v. 34, 1-81.

Lowell, J.P. and Guilbert, J.M., 1970, Lateral and vertical alteration-mineralization zoning in porphyry copper deposits. Economic Geology, v. 65, 373-408.

Martin, M.W., Dilles, J.H., and Proffett, J.M., 1999, U-Pb geochronologic constraints for the Butte porphyry system. Geological Society of America, Annual Meeting 1999, Denver, Abstract with Programs, v. 31, p. A-380.

Matthäi, S.M. and Roberts, S.G., 1999, Complex system platform CSP3D3.0 user's guide. Swiss Federal Institute of Technology (ETH) Zurich, 106 pages.

Meyer, C., Shea, E.P., Goddard, C.C., and staff, 1968, Ore deposits at Butte, MT. in Ridge, D. J. (ed.) Ore deposits of the United States 1933-1967 (Graton-Sales Vol.): v. 2, 1363-1416.

Moreno, L., Neretnieks, I., and Eriksen, T., 1985, Analysis of some laboratory tracer runs in natural fissures. Water Resources Research, v. 21, 951-958.

Moreno, L., Tsang, Y.W., Tsang, C.F., Hale, F.V., and Neretnieks, I., 1988, Flow and tracer transport in a single fracture: A stochastic model and its relation to some field observations. Water Resources Research, v. 24, 2033-2048.

Neretnieks, I., 1980, Diffusion in the rock matrix: an important factor in radionuclide retardation? Journal of Geophysical Research, v. 85, 4379-4397.

Neretnieks, I. and Rasmuson, A., 1984, An approach to modelling radionuclide migration in a medium with strongly varying velocity and block sizes along the flow path. Water Resources Research, v. 20, 1823-1836.

Norton, D. and Taylor, H.P. Jr., 1979, Quantitative simulation of the hydrothermal systems of crystallizing magmas on the basis of transport theory and oxygen isotope data: Skaergaard intrusion. Journal of Petrology, v. 20, 421-486.

Oelkers, E.H., 1996, Physical and chemical properties of rocks and fluids for chemical mass transport calculations. In: Lichtner, P. C., Steefel, C. I., and Oelkers, E. H. (eds.), Reactive Transport in Porous Media. Reviews in Mineralogy, v. 34, 131-191.

Ohlsson, Y. and Neretnieks, I., 1995, Literature survey of matrix diffusion theory and of experiments and data including natural analogues. Swedish Nuclear Fuel and Waste Management Corporation, SKB Technical Report 95-12, Sweden, 89 pages.

Phillips, O.M., 1991, Flow and reactions in permeable rocks. Cambridge University Press, 277 pages.

Proffett, J.M., 1973, The structure of the Butte District, Montana. Guide Book for the Butte Field Meeting of the Society of Economic Geologists 1973, p. G 1-12.

Reed, M.H., 1979, Butte District Early Stage Geology. Anaconda Company report, 40 pages., 24 plates and figures.

Reed, M.H., 1997, Hydrothermal alteration and its relationship to ore fluid composition. In: Barnes, H.L. (ed.), Geochemistry of hydrothermal ore deposits, 3rd edition, 303-365. John Wiley & Sons.

Reed, M.H., 1998, Calculations of simultaneous chemical equilibria in aqueous-mineral-gas systems and its application to modeling hydrothermal processes. In: Richards, J.P. and Larson, P.B. (eds.), Techniques in hydrothermal ore deposits geology. Reviews in Economic Geology, v. 10, 109-124.

Reed, M.H. and Palandri, J., 1999, Soltherm.HIP data base. A compilation of thermodynamic data from 25°C to 500°C for aqueous species, minerals and gases. University of Oregon, 36 pages.

Roberts, S.A., 1975, Early hydrothermal alteration and mineralization in the Butte district, Montana. Unpublished Ph.D. thesis, Harvard University.

Sales, R.H. and Meyer, C., 1948, Wallrock alteration, Butte, Montana. Am. Inst. Min. Metal. Eng. Trans., v. 178, 9-35.

Sales, R.H. and Meyer, C., 1949, Results for preliminary studies of vein formation at Butte, Montana. Economic Geology, v. 44, 465-484.

Sheppard, M.F. and Taylor, H.T., 1974, Hydrogen and Oxygen Evidence for the Origins of Water in the Boulder Batholith and the Butte Ore Deposits, Montana. Economic Geology, v.69, 926-946.

Smedes, H.W., 1973, Regional Setting and general Geology of the Boulder Batholith, Montana. Guide Book for the Butte Field Meeting of the Society of Economic Geologists 1973, p. A 1-6.

Snee, L., Miggins, D., Geissman, J., Reed, M.H., Dilles, J.H., and Zhang, L., 1999, Thermal history of the Butte porphyry system, Montana. Geological Society of America, Annual Meeting 1999, Denver, Abstract with Programs, v. 31, p. A-380.

Soler, J.M. and Lasaga, A.C., 1998, An advection-dispersion-reaction model of bauxite formation. Journal of Hydrology, v. 209, 311-330.

Steefel, C.I. and Lasaga, A.C., 1992 Putting transport into water-rock interaction models. Geology, v. 20, 680-684.

Steefel, C.I. and Lasaga, A.C., 1994, A coupled model for transport of multiple chemical species and kinetic precipitation / dissolution reactions with application to reactive flow in single phase hydrothermal systems. American Journal of Science, v. 294, 529-592.

Steefel, C.I. and Lichtner P.C., 1994, Diffusion and reaction in rock matrix bordering a hyperalkaline fluid-filled fracture. Geochimica et Cosmochimica Acta, v. 58, 3592-3612.

Steefel, C.I. and MacQuarrie, K.T.B., 1996, Approaches to modeling of reactive transport in porous media. In: Lichtner, P. C., Steefel, C. I., and Oelkers, E. H. (eds.), Reactive Transport in Porous Media. Reviews in Mineralogy, v. 34, 83-129.

Steefel, C.I. and Lichtner, P.C., 1998a, Multicomponent reactive transport in discrete fractures: I. Controls on reaction front geometry. Journal of Hydrology, v. 209, 186-199.

Steefel, C.I. and Lichtner, P.C., 1998b, Multicomponent reactive transport in discrete fractures: II. Infiltration of hyperalkaline groundwater at Maqarin, Jordan, a natural analogue site. Journal of Hydrology, v. 209, 200-224.

Valocchi, A.J. and Malmstead, M., 1992, Accuracy of operator splitting for advection-dispersion-reaction problems. Water Resources Research, v. 28, 1471-1476.

Van Barkel, J. and Heertjes, P.M., 1974, Analysis of diffusion in macroporous media in terms of a porosity, a tortuosity and a constrictivity factor. International Journal of Heat Mass Transfer, v 17, 1082-1103.

Wagner, W. and Kruse, A., 1998, Properties of water and steam. Springer Verlag, 354 pages.

Wells, J.T. and Ghiorso, M.S., 1991, Coupled fluid flow ad reaction in mid-ocean ridge hydrothermal systems: The behavior of silica. Geochimica et Cosmochimica Acta, v. 55, 2467-2481.

Yeh, H.C. and Tripathi, V.S., 1989, A critical evaluation of recent developments in hydrogeochemical transport models of reactive multichemical components. Water Resources Research, v. 25, 93-108.

Yeh, H.C. and Tripathi, V.S., 1991, A model for simulating transport of reactive multispecies components: Model development and demonstration. Water Resources Research, v. 27. 3075-3094.

Zhang, L., Dilles, J.H., and Field, C.W., 1999, Oxygen and hydrogen isotope geochemistry of pre-Main Stage porphyry Cu-Mo mineralization at Butte, Montana. Geological Society of America, Annual Meeting 1999, Denver, Abstract with Programs, v. 31, p. A-381.

Zysset, A. and Stauffer, F., 1992, Modeling of microbial processes in groundwater infiltration systems. In Russell, T.F., Ewing, R.E., Brebbia, C.A., Gray, W.G., and Pinder, G.F. (eds.): Mathematical Modelling in Water Resources. Computational Mechanics Publications, Billerica, Massachusetts.

Zysset, A., Stauffer, F, and Dracos, T., 1994, Modeling of chemically reactive groundwater transport. Water Resources Research, v. 30, 2217-2228.

CHAPTER IV

CONCLUDING REMARKS

In this thesis, a model was introduced to explain the temporal and spatial simulation of the sericitic pre-Main Stage hydrothermal alteration at Butte, Montana. The model included mathematical descriptions of the physics of multi-component diffusion and reaction under stationary state conditions, vein geology, geochemical modeling, and reactive transport simulations of a hydrothermal fluid diffusing into a rock matrix adjacent to a fracture and chemically altering the rock composition. The model successfully predicted the development of the observed hydrothermal alteration at Butte, Montana. The model is also applicable to many other porphyry copper deposits around the world that contain alteration zones similar to the sericitic pre-Main Stage alteration at Butte.

From the mathematical description of the quasi-stationary state approximation (Lichtner, 1988; 1991), it follows that mineral reaction fronts have narrow widths under transport controlled conditions. Furthermore, the mineral reaction fronts advance as the square root of time and also depend on the concentration gradient and consequently the flux across the reaction front. This is important for the evolution of a sequence of reaction fronts. Each mineral reaction front advances at a specific rate. Since every front advances as the square root of time, the relative movement of the fronts to each other is time-independent and is solely a function of the concentration gradient across the reaction front. Hence the

relative locations of the reaction fronts remain constant once the pattern of reaction fronts is fully developed. The width of a mineral reaction zone can increase or decrease if its bounding reaction fronts advance at different rates. Furthermore, it follows that the ratio of the widths of two reaction zones remains constant. Since reaction fronts are narrow under transport-limited conditions, the edge of the unaltered rock is characterized by a sharp transition. The results of reactive transport modeling of the sericitic pre-Main Stage alteration at Butte show the behavior predicted by the properties of the quasi-stationary state approximation. The mineral reaction fronts advance at rates that are constant relative to each other and the mineral reaction zones increase in width. Owing to the decoupling of the reaction and transport step in the model, the reaction fronts are not as narrow as predicted and as observed in natural samples of mineral alteration zones.

A further analysis of the quasi-stationary state approximation shows that the initial mineral mass can be scaled by a factor F_m, which is less than one. If the mineral mass is scaled by a factor F_m, time in the reactive transport simulation must be scaled by the factor F^*. The factor F^* is a function of F_m, and the volume of the fluid V_f and the mineral V_m. Scaling the distance in the simulation by the square root of F^* is also equivalent to scaling time by F^*.

Mass scaling, however, increases the numerical inaccuracy in the simulations. The numerical inaccuracy causes incorrect locations of the reaction fronts although the relative location of the reaction fronts to each other are not affected. Furthermore, the time necessary to establish the full sequence of reaction

fronts cannot be determined exactly. The decoupling of the reaction and transport steps probably causes the numerical problem because changing the time-steps in the simulations that use identical parameters also yields different locations for the reaction fronts and different time frames. This makes the application of the SIA method currently problematic for reactive transport simulations of geologic systems because the absolute timing and location of a sequence of reaction fronts cannot be calculated exactly. The relative locations of the mineral reaction fronts are not affected by mass-scaling or the use of different time-steps. Many physical and chemical parameters in fossil hydrothermal systems, however, are not well known and may introduce a bigger inaccuracy than the numerical problem of the SIA method. Scaling mineral masses was successfully applied in the reactive transport simulations of the sericitic pre-Main Stage alteration.

Reactive transport simulations of the gray sericitic and sericite with remnant biotite zones at Butte show that a reducing, low salinity, and highly acidic fluid can produce the sequence of alteration envelopes at Butte probably during a time span less than one hundred years. Hydrothermal alteration has little effect on the porosity of the wall-rock, and solute transport is therefore not influenced by significant changes in diffusivity. However, the hydrolysis and precipitation of minerals affect solute transport, because new concentration gradients are imposed on the fluid.

The sequence of mineral reaction fronts in the wall-rock depends on the pH, which increases with increasing distance into the matrix, and on the concentration

of the other reactive solutes the particular mineral reactions. Muscovite, quartz, pyrite, and anhydrite replace feldspar, biotite, amphibole, and magnetite of the Butte Quartz Monzonite close to the fracture. This mineral assemblage characterizes the gray sericitic alteration zone. Biotite is the first mineral of the Butte Quartz Monzonite that becomes stable into the matrix and therefore marks the transition from the gray sericitic to the sericite with remnant biotite zone, forming an inner gray sericitic and an outer sericite with remnant biotite alteration envelope. The occurrence of fresh plagioclase marks the edge of the unaltered Butte Quartz Monzonite in natural samples. The plagioclase front, however, trails the microcline front in the simulations. This is probably caused by an error in the thermodynamic data for the hydrolysis of anorthite.

Since the properties of multi-component diffusion and reaction require that reaction fronts retain their relative locations to each other, the biotite dissolution front always marks the transition between gray sericitic and sericite with remnant biotite zone. Furthermore, the plagioclase dissolution front always marks the edge of the unaltered Butte Quartz Monzonite in natural samples. As both of those reaction fronts advance into the matrix, the gray sericitic and sericite with remnant biotite zones grow in width. Their widths maintain a constant ratio relative to each other unless the gray sericite zone is not fully developed at early times. From the physical properties of reactive transport in fractures, it follows that the alteration halos decrease in width along the fracture because diffusion or reactive solutes in

the rock matrix occurs at a lower rate then advection in the fracture, which can cause wedging of the alteration zones (Steefel and Lichtner, 1998a).

These observations can also be applied to those porphyry copper deposits around the world that comprise hydrothermal alteration zones similar to the sericitic pre-Main Stage alteration at Butte, Montana. The results therefore offer insight about the temporal and spatial evolution of a very common type of hydrothermal alteration envelopes. It has also been the first time that the evolution of alteration zones during high temperature and pressure was studied quantitatively. It is planned to implement the quasi-stationary state approximation into CSP3D3.0. This allows the efficient simulation of non-isothermal multi-phase systems, hydrothermal alteration in fractured networks, and a more exact calculation of the composition of the hydrothermal fluid.

BIBLIOGRAPHY

Aagaard, P. and Helgeson, H.C., 1982, Thermodynamic and kinetic constrains in reaction rates among minerals and aqueous solutions, I. Theoretical considerations. American Journal of Science, v. 282, 237-285.

Beaudoin, G. and Therrien, R., 1999, Sources and drains; major controls of hydrothermal fluid flow in the Kokanee Range, British Columbia, Canada. Geology, v.27, 883-886.

Blount, C.W. and Dickson, F.W., 1968, The solubility of anhydrite ($CaSO_4$) in $NaCl-H_2O$ from 100 to 450 degrees C and 1 to 1000 bars. Geochimica et Cosmochimica Acta, v. 33, 227-245.

Brimhall, G.H., 1977, Early fracture controlled disseminated mineralization at Butte, Montana. Economic Geology, v. 72, 37-59.

Brimhall, G.H., 1979, Lithologic determination of mass transfer mechanisms of multiple-stage porphyry copper mineralization at Butte, MT: Vein formation by hypogene leaching and enrichment of potassium-silicate. Economic Geology v. 74, 556-590.

Brimhall, G.H., 1980, Deep hypogene oxidation of porphyry copper potassium-silicate protore at Butte, Montana: A theoretical evaluation of the copper remobilization hypothesis. Economic Geology, v. 75, 348-409.

Brimhall, G.H. and Ghiorso, M.S., 1983, Origin and ore-forming consequences of the advanced argillic alteration process in hypogene environments by magmatic gas contamination of meteoric fluids. Economic Geology, v. 78, 73-90.

Brown, J.G., Bassett, R.L., and Glynn, P.D., 1998, Analysis and simulation of reactive transport of metal contaminants in ground water in Pinal Creek, Arizona. Journal of Hydrology, v. 209, 225-250.

Cathles, L.M., 1983, An analysis of the hydrothermal system responsible for deposition of massive sulfide deposition in the Hokuroku Basin of Japan. Economic Geology Monograph 5, 439-487.

Cussler, E.L., 1996, Diffusion: Mass transfer in fluid Systems. Cambridge University Press, 525 pages.

Désilets, M., Proulx, P., and Soucy, G., 1997, Modeling of multicomponent diffusion in high temperature flows. International Journal Heat Mass Transfer, v. 40, 4273-4278.

Dilles, J.H. and Einaudi, M.T., 1992, Wall-rock alteration and hydrothermal flow paths about the Ann-Mason porphyry copper deposit, Nevada--A 6 km vertical reconstruction. Economic Geology, v. 87, 1963-2001.

Domenico, P.A. and Schwarz, F.W., 1990, Physical and Chemical Hydrogeology. John Wiley and Sons, 824 pages.

Engesgaard, P. and Kipp, K.L., 1992, A geochemical model for redox-controlled movement of mineral fronts in groundwater-flow systems: A case of nitrate removal by oxidation of pyrite. Water Resources Research, v. 28, 2829-2843.

Geiger, S., 2000, Reactive transport modeling in discrete fractures: Applications to the formation of sericitic hydrothermal alteration at Butte, Montana. MS Thesis, Dept. of Geosciences, Oregon State University, 124 pages.

Getahun, A., 1994, Fluid-rock reaction and mineralization in two high-level volcanic settings: Augustine Fumaroles and the Summitville acid-sulfate copper-gold deposit. Ph.D. dissertation, University of Oregon, 331pages.

Glynn, P.D. and Brown, J.G., 1996, Reactive transport modeling of acidic metal-contaminated groundwater at a site with sparse spatial information. In: Lichtner, P.C., Steefel, C.I., and Oelkers, E.H. (eds.), Reactive Transport in Porous Media. Reviews in Mineralogy, v. 34, 377-438.

Gustafson, L.N. and Hunt, J.P., 1975, The porphyry copper deposits at El Salvador, Chile. Economic Geology, v.70, 857-912.

He, W., Zhengyu, B., and Tieping, L., 1999, One-dimensional reactive transport models of alteration in the Tongchang porphyry copper deposit, Dexing District, Jiangxi Province, China. Economic Geology, v. 94, 307-323.

Helgeson, H.C., 1979, Mass transfer among minerals and hydrothermal solutions. In: Barnes, H.L. (ed.), Geochemistry of hydrothermal ore deposits, 2nd edition, 421-469. John Wiley & Sons.

Houston, R.A., 1999, The Butte District, Montana - New field data and reassessment of post-mineral structural tilting. Geological Society of America, Annual Meeting 1999, Denver, Abstract with Programs, v. 31, p. A-382.

Johnson, J.W., Knauss, K.G., Glassley, W.E., DeLoach, L.D., and Tompson, A.F.B., 1998, Reactive transport modeling of plug-flow reactor experiments: quartz and tuff dissolution at 240°C. Journal of Hydrology, v. 209, 81-111.

Klepper, M.R., 1973, Geology of the Southern Part of the Boulder Batholith. Guide Book for the Butte Field Meeting of the Society of Economic Geologists 1973, p. B 1-5.

Knopf, A., 1957, The Boulder Batholith of Montana. American Journal of Science, v. 255, 81-103.

Lasaga, A.C., 1984, Chemical kinetics of water-rock interactions. Journal Geophysical Research, v. 89, 4009-4025.

Lasaga, A.C. and Rye, D.M., 1993, Fluid flow and chemical reaction kinetics in metamorphic systems. American Journal of Science, v. 293, 2169-2175.

Lichtner, P.C., 1985, Continuum model for simultaneous chemical reactions and mass transport in hydrothermal systems. Geochimica et Cosmochimica Acta, v. 49, 779-800.

Lichtner, P.C., Oelkers, E. H., and Helgeson, H.C., 1986, Interdiffusion with multiple precipitation / dissolution reactions: Transient model and steady-state limit. Geochimica et Cosmochimica Acta, v. 50, 1951-1966.

Lichtner, P.C., 1988, The quasi-stationary state approximation to coupled mass transport and fluid-rock interaction in a porous medium. Geochimica et Cosmochimica Acta, v. 52, 143-165.

Lichtner, P.C., 1991, The quasi-stationary state approximation to fluid/rock interaction: local equilibrium revisited. In: Ganguly, J. (ed.) Diffusion, atomic ordering and mass transport. Advances in Physical Geochemistry, v. 8, 454-562. Springer Verlag.

Lichtner, P.C., 1992, Time-space continuum description of fluid / rock interaction. Water Resources Research, v. 28, 3135-3155.

Lichtner, P.C. and Biino G.G., 1992, A first principles approach to supergene enrichment of porphyry copper protore. I. Cu-Fe-S-H_2O subsystem. Geochimica et Cosmochimica Acta, v. 56, 3987-4013.

Lichtner, P.C., 1993, Scaling properties of time-space kinetic mass transport equations and the local equilibrium limit. American Journal of Science, v. 293, 257-296.

Lichtner, P.C. and Balashov, V.N., 1993, Metasomatic zoning: appearance of ghost zones in the limit of pure advective mass transport. Geochimica et Cosmochimica Acta, v. 57, 369-387.

Lichtner, P.C., 1996, Continuum formulation of multicomponent-multiphase reactive transport. In: Lichtner, P.C., Steefel, C.I., and Oelkers, E.H. (eds.), Reactive Transport in Porous Media. Reviews in Mineralogy, v. 34, 1-81.

Lowell, J.P. and Guilbert, J.M., 1970, Lateral and vertical alteration-mineralization zoning in porphyry copper deposits. Economic Geology, v. 65, 373-408.

Martin, M.W., Dilles, J.H., and Proffett, J.M., 1999, U-Pb geochronologic constraints for the Butte porphyry system. Geological Society of America, Annual Meeting 1999, Denver, Abstract with Programs, v. 31, p. A-380.

Matthäi, S.M. and Roberts, S.G., 1999, Complex system platform CSP3D3.0 user's guide. Swiss Federal Institute of Technology (ETH) Zurich, 106 pages.

Meyer, C., Shea, E.P., Goddard, C.C., and staff, 1968, Ore deposits at Butte, MT. in Ridge, D. J. (ed.) Ore deposits of the United States 1933-1967 (Graton-Sales Vol.): v. 2, 1363-1416.

Moreno, L., Neretnieks, I., and Eriksen, T., 1985, Analysis of some laboratory tracer runs in natural fissures. Water Resources Research, v. 21, 951-958.

Moreno, L., Tsang, Y.W., Tsang, C.F., Hale, F.V., and Neretnieks, I., 1988, Flow and tracer transport in a single fracture: A stochastic model and its relation to some field observations. Water Resources Research, v. 24, 2033-2048.

Neretnieks, I., 1980, Diffusion in the rock matrix: an important factor in radionuclide retardation? Journal of Geophysical Research, v. 85, 4379-4397.

Neretnieks, I. and Rasmuson, A., 1984, An approach to modelling radionuclide migration in a medium with strongly varying velocity and block sizes along the flow path. Water Resources Research, v. 20, 1823-1836.

Norton, D. and Taylor, H.P. Jr., 1979, Quantitative simulation of the hydrothermal systems of crystallizing magmas on the basis of transport theory and oxygen isotope data: Skaergaard intrusion. Journal of Petrology, v. 20, 421-486.

Novak, C.F., Schechter, R.S., and Lake, L.W., 1989, Diffusion and solid dissolution/precipitation in permeable media. AIChE Journal, v.35, 1057-1072.

Oelkers, E.H., 1996, Physical and chemical properties of rocks and fluids for chemical mass transport calculations. In: Lichtner, P. C., Steefel, C. I., and Oelkers, E. H. (eds.), Reactive Transport in Porous Media. Reviews in Mineralogy, v. 34, 131-191.

Ohlsson, Y. and Neretnieks, I., 1995, Literature survey of matrix diffusion theory and of experiments and data including natural analogues. Swedish Nuclear Fuel and Waste Management Corporation, SKB Technical Report 95-12, Sweden, 89 pages.

Phillips, O.M., 1991, Flow and reactions in permeable rocks. Cambridge University Press, 277 pages.

Proffett, J.M., 1973, The structure of the Butte District, Montana. Guide Book for the Butte Field Meeting of the Society of Economic Geologists 1973, p. G 1-12.

Reed, M.H., 1979, Butte District Early Stage Geology. Anaconda Company report, 40 pages., 24 plates and figures.

Reed, M.H., 1997, Hydrothermal alteration and its relationship to ore fluid composition. In: Barnes, H.L. (ed.), Geochemistry of hydrothermal ore deposits, 3rd edition, 303-365. John Wiley & Sons.

Reed, M.H., 1998, Calculations of simultaneous chemical equilibria in aqueous-mineral-gas systems and its application to modeling hydrothermal processes. In: Richards, J.P. and Larson, P.B. (eds.), Techniques in hydrothermal ore deposits geology. Reviews in Economic Geology, v. 10, 109-124.

Reed, M.H. and Palandri, J., 1999, Soltherm.HIP data base. A compilation of thermodynamic data from 25°C to 500°C for aqueous species, minerals and gases. University of Oregon, 36 pages.

Roberts, S.A., 1975, Early hydrothermal alteration and mineralization in the Butte district, Montana. Unpublished Ph.D. thesis, Harvard University.

Sales, R.H. and Meyer, C., 1948, Wallrock alteration, Butte, Montana. Am. Inst. Min. Metal. Eng. Trans., v. 178, 9-35.

Sales, R.H. and Meyer, C., 1949, Results for preliminary studies of vein formation at Butte, Montana. Economic Geology, v. 44, 465-484.

Sheppard, M.F. and Taylor, H.T., 1974, Hydrogen and Oxygen Evidence for the Origins of Water in the Boulder Batholith and the Butte Ore Deposits, Montana. Economic Geology, v.69, 926-946.

Skagius, K. and Neretnieks, I., 1986, Porosities and diffusivities of some nonsorbing species in crystalline rocks. Water Resources Research, v. 22, 389-398.

Smedes, H.W., 1973, Regional Setting and general Geology of the Boulder Batholith, Montana. Guide Book for the Butte Field Meeting of the Society of Economic Geologists 1973, p. A 1-6.

Snee, L., Miggins, D., Geissman, J., Reed, M.H., Dilles, J.H., and Zhang, L., 1999, Thermal history of the Butte porphyry system, Montana. Geological Society of America, Annual Meeting 1999, Denver, Abstract with Programs, v. 31, p. A-380.

Soler, J.M. and Lasaga, A.C., 1998, An advection-dispersion-reaction model of bauxite formation. Journal of Hydrology, v. 209, 311-330.

Steefel, C.I. and Lasaga, A.C., 1992 Putting transport into water-rock interaction models. Geology, v. 20, 680-684.

Steefel, C.I. and Lasaga, A.C., 1994, A coupled model for transport of multiple chemical species and kinetic precipitation / dissolution reactions with application to reactive flow in single phase hydrothermal systems. American Journal of Science, v. 294, 529-592.

Steefel, C.I. and Lichtner P.C., 1994, Diffusion and reaction in rock matrix bordering a hyperalkaline fluid-filled fracture. Geochimica et Cosmochimica Acta, v. 58, 3592-3612.

Steefel, C.I. and MacQuarrie, K.T.B., 1996, Approaches to modeling of reactive transport in porous media. In: Lichtner, P. C., Steefel, C. I., and Oelkers, E. H. (eds.), Reactive Transport in Porous Media. Reviews in Mineralogy, v. 34, 83-129.

Steefel, C.I. and Yabusaki, S.B., 1996, OS3D/GIMRT, Software for Multicomponent-Multidimensional Reactive Transport, Users Manual and Programmer's Guide. PNL-11166, Pacific Northwest Laboratory, Richland, Washington.

Steefel, C.I. and Lichtner, P.C., 1998a, Multicomponent reactive transport in discrete fractures: I. Controls on reaction front geometry. Journal of Hydrology, v. 209, 186-199.

Steefel, C.I. and Lichtner, P.C., 1998b, Multicomponent reactive transport in discrete fractures: II. Infiltration of hyperalkaline groundwater at Maqarin, Jordan, a natural analogue site. Journal of Hydrology, v. 209, 200-224.

Valocchi, A.J. and Malmstead, M., 1992, Accuracy of operator splitting for advection-dispersion-reaction problems. Water Resources Research, v. 28, 1471-1476.

Van Barkel, J. and Heertjes, P.M., 1974, Analysis of diffusion in macroporous media in terms of a porosity, a tortuosity and a constrictivity factor. International Journal of Heat Mass Transfer, v 17, 1082-1103.

Viswanathan, H.S., Robinson, B.A., Valocchi, A.J., and Triay, I.R., 1998, A reactive transport model of neptunium migration from the potential repository at Yucca Mountain. Journal of Hydrology, v. 209, 251-280.

Wagner, W. and Kruse, A., 1998, Properties of water and steam. Springer Verlag, 354 pages.

Wang, Y. and Van Capellen, P., 1996, A multicomponent reactive transport model of early diagenesis: application to redox cycling in coastal marine sediments. Geochimica et Cosmochimica Acta, v. 60, 2993-3014.

Wells, J.T. and Ghiorso, M.S., 1991, Coupled fluid flow ad reaction in mid-ocean ridge hydrothermal systems: The behavior of silica. Geochimica et Cosmochimica Acta, v. 55, 2467-2481.

Wood, B.D., Ginn, T.R., and Dawson, C.N., 1995, Effects of microbial metabolic lag in contaminant transport and biodegradation modeling. Water Resources Research, v. 31., 553-563.

Wood, W.W., 1997, Fluxes: A new paradigm for geologic education? Groundwater, v.35, 1.

Yeh, H.C. and Tripathi, V.S., 1989, A critical evaluation of recent developments in hydrogeochemical transport models of reactive multichemical components. Water Resources Research, v. 25, 93-108.

Yeh, H.C. and Tripathi, V.S., 1991, A model for simulating transport of reactive multispecies components: Model development and demonstration. Water Resources Research, v. 27. 3075-3094.

Zhang, L., Dilles, J.H., and Field, C.W., 1999, Oxygen and hydrogen isotope geochemistry of pre-Main Stage porphyry Cu-Mo mineralization at Butte, Montana. Geological Society of America, Annual Meeting 1999, Denver, Abstract with Programs, v. 31, p. A-381.

Zysset, A. and Stauffer, F., 1992, Modeling of microbial processes in groundwater infiltration systems. In Russell, T.F., Ewing, R.E., Brebbia, C.A., Gray, W.G., and Pinder, G.F. (eds.): Mathematical Modelling in Water Resources. Computational Mechanics Publications, Billerica, Massachusetts.

Zysset, A., Stauffer, F, and Dracos, T., 1994, Modeling of chemically reactive groundwater transport. Water Resources Research, v. 30, 2217-2228.

APPENDIX

CALCULATION OF DIFFUSIVITIES FROM POROSITIES IN CRYSTALLINE ROCKS

Introduction

Van Barkel and Heertjes (1974) have discussed empirical expressions for the relation between the pore diffusivity and porosity for high-porosity media. Skagius and Neretnieks (1986) have also derived an empirical relation between pore diffusivity and porosity for crystalline rocks and high-porosity media. The relation discussed by Skagius and Neretnieks (1986) suggests that pore diffusivity increases linearly with porosity. An explicit expression for the relation between pore diffusivity and porosity in low-porosity rocks has not been derived so far. Understanding the feedback between solute transport and changes in porosity caused by mineral precipitation and dissolution is of key interest in reactive transport simulations (c.f., Lichtner, 1996; Oelkers, 1996; Steefel and MacQuarrie, 1996). A relation between pore diffusivity and porosity in low-porosity rocks is specifically helpful for reactive transport models that include hydrothermal alteration of crystalline rocks (Geiger, 2000) or metamorphism (Lasaga and Rye, 1993).

Diffusion of solutes in porous media differs from diffusion in an aqueous solution because the structure of the pore space alters the diffusive behavior of the solute. The solute interacts chemically and physically with the pore walls of the porous media. Chemical interactions can involve sorption of the solutes on pore-

wall surfaces and mineral reactions of the solutes. Non-straight diffusion pathways (tortuosity), collision of especially larger solutes with the pore walls (restrictivity), and drag on the solutes caused by nearby pore-walls hinder diffusion physically (Cussler, 1996). Porosity, tortuosity, and restrictivity are therefore parameters that define the geometry of the pore space and describe the physical interaction of the solute with the pore space. With the exception of porosity, however, these parameters are very difficult to measure for geologic media. Deriving a formulation that allows the calculation of the pore diffusivity from porosity only is therefore helpful for any reactive transport model.

Mathematical Description

Ohlsson and Neretnieks (1995) describe diffusion of a single non-reactive solute within the porous media as the porous diffusivity D_p

$$D_p = D_{aq} \frac{\delta}{\tau^2} \qquad \text{(A1)}$$

The aqueous diffusivity is D_{aq}. Both, D_p and D_{aq}, have units of $[L^2 T^{-1}]$. The restrictivity of the porous media is δ. The tortuosity is τ, and the porosity is ϕ. Restrictivity and tortuosity have units of $[L^2]$, while porosity is dimensionless [-].

Diffusion of a single non-reactive solute from an aqueous solution into the porous media is described as the effective diffusivity D_e (Ohlsson and Neretnieks, 1995)

$$D_e = D_{aq} \frac{\delta}{\tau^2} \phi \tag{A2}$$

The product of porosity, tortuosity, and restrictivity is also known as the dimensionless formation factor f_m (Ohlsson and Neretnieks, 1995)

$$f_m = \delta \phi \tau^{-2} \tag{A3}$$

Since tortuosity and restrictivity can vary for the same porosity value, diffusivities cannot simply be calculated from porosity values only. Skagius and Neretnieks (1986) and Oelkers (1996) discuss a first approximation commonly applied in reactive transport simulations to approximate D_p where the formation factor for a given porosity is defined as

$$f_m = \phi^2 \tag{A4}$$

which implies that the pore diffusivity increases linearly with porosity since

$$D_p = D_{aq} \frac{\delta}{\tau^2} = D_{aq} \frac{f_m}{\phi} = D_{aq} \phi \tag{A5}$$

Empirical Relations

Van Barkel and Heertjes (1974) compared several empirical and theoretical relations between the matrix factor and porosity for diffusion of a single non-reactive solute. Some of those relationships are plotted in Figure A1. Most of the relations compiled by Van Barkel and Heertjes (1974) are derived for high-porosity media.

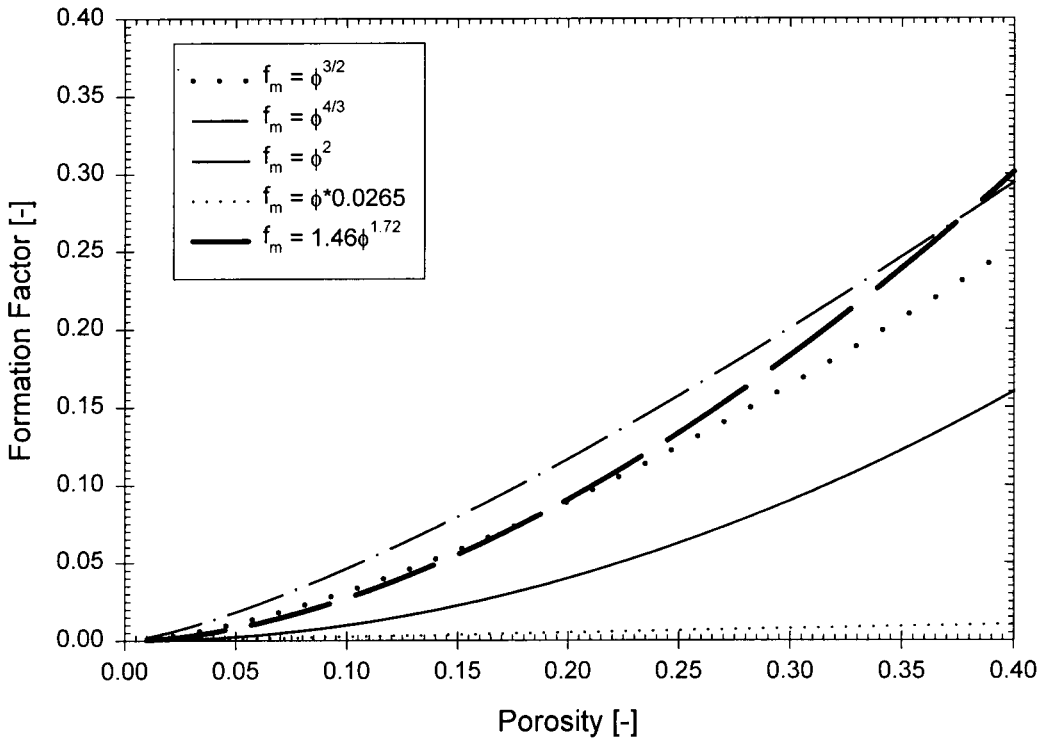

Figure A1. Theoretical and empirical relations for the calculation of the formation factor f_m from porosity ϕ for the diffusion of a single non-reactive solute (after Van Barkel and Heertjes, 1974). The thick dashed line ($f_m = 1.47\phi^{1.72}$) is an empirical relation from a non-linear best fit ($R^2 = 0.5$) through formation factor data in low-porosity crystalline rocks, as given in Ohlsson and Neretnieks (1995).

Ohlsson and Neretnieks (1995) compiled measurements of the formation factor for a variety of low porous crystalline rocks from Sweden. Those formation factors are plotted versus their associated porosities at very low-porosity values in Figure A2. The graph displays that the relationships discussed in Van Barkel and Heertjes (1974) are not in good agreement with the data measured by Ohlsson and Neretnieks (1995) (Fig. A2). Ohlsson and Neretnieks (1995) took their measurements in low-porosity crystalline rocks while the relationships discussed by Van Barkel and Heertjes are derived for high-porosity media.

A non-linear best-fit line through the formation factor data from Ohlsson and Neretnieks (1995) gives the following relation at low porosities ($R^2 = 0.5$)

$$f_m = 1.42\phi^{1.72} \tag{A6}$$

Combining equations (A2), (A3), and (A6) yields a formulation for the pore diffusivity D_p for a single non-reactive solute in low porous geologic media

$$D_p = D_{aq}\frac{\delta}{\tau^2} = D_{aq}\frac{f_m}{\phi} = \frac{D_{aq}1.47\phi^{1.72}}{\phi} \tag{A7}$$

or simplified as

$$D_p = D_{aq}1.47\phi^{0.72} \tag{A8}$$

Equation A8 suggests that at low porosities the pore diffusivity increases non linearly with an increasing porosity.

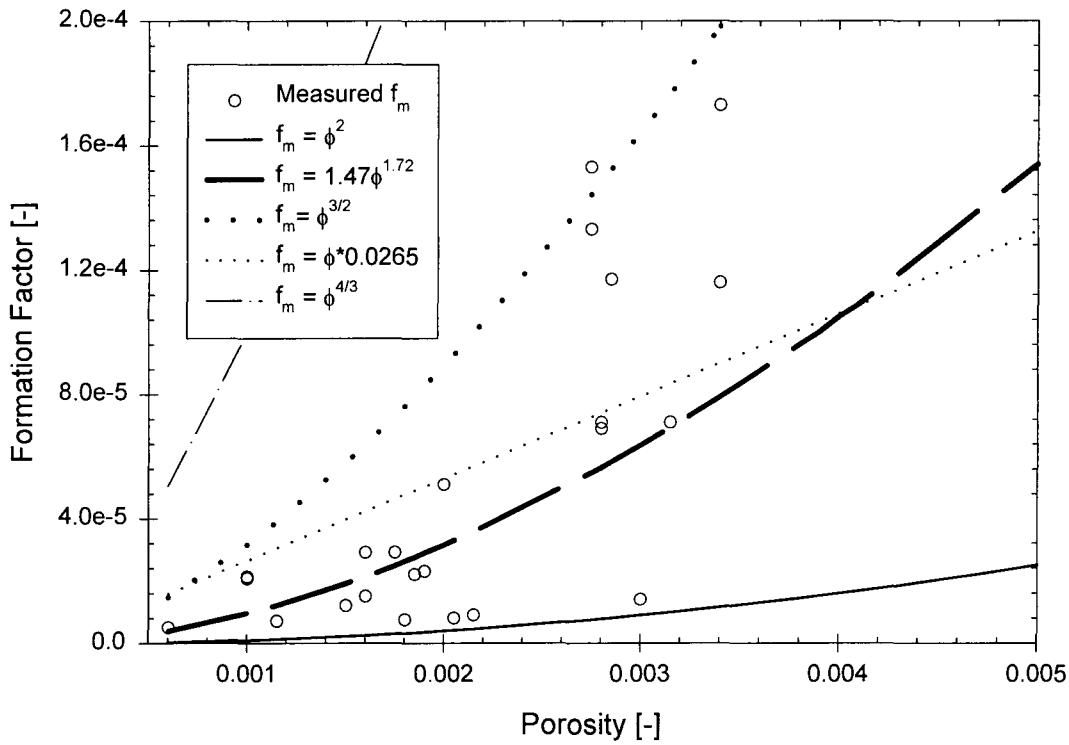

Figure A2. Close-up at low porosities of the theoretical and empirical relations between the formation factor f_m and porosity ϕ and comparison with formation factors measured by Ohlsson and Neretnieks (1995) in crystalline rocks. For very low porosity values, the relation $f_m = \phi*0.0265$ (thin dotted line) also appears to be a good fit but yields formation factor values that are too low at higher porosities if compared to all other relations (Fig. A1). The commonly used relation (Oelkers, 1996) $f_m = \phi^2$ (solid line) seems to predict formation factors that are too low at very low porosities, while the relations $f_m = \phi^{4/3}$ (dashed-dotted line) and $f_m = \phi^{3/2}$ (thick dotted line) give formation factors that are too high. The expression $f_m = 1.47\phi^{1.72}$ (thick dashed line) yields reasonable results at low porosities, but over-predicts the formation factor at porosities above 40% (Fig. A2).

Discussion of Different Empirical Relations

The linear expression $f_m = \phi * 0.0265$ appears to be another good fit at low porosities, but yields formation factors at high porosities that are significantly lower than those calculated from other relations (Fig. A1). The expressions $f_m = \phi^{3/2}$ and $f_m = \phi^{4/3}$ over-predict the formation factor, while the expression $f_m = \phi^2$ (Skagius and Neretnieks, 1986) seems to give formation factors that are too low (Fig. A2). In comparison to other relations discussed by Van Barkel and Heertjes (1974), the expression $f_m = 1.42\ \phi^{1.72}$ appears to yield reasonable values for the formation factor up to porosities of 40%. For porosities larger than 40%, the formation factor would be predicted too high (Fig. A1). Changes in porosity during hydrothermal alteration of igneous rocks are rather small and porosities should not become larger than 40% (Geiger, 2000). The relation $f_m = 1.42\ \phi^{1.72}$ should therefore hold if applied to calculate diffusion coefficients in low-porosity crystalline rocks.

Diffusivities calculated from porosity values for different empirical relationships are shown in Figure A3. This graph shows the non-linear relation between pore diffusivity and porosity discussed in equation A8 and also implies that the pore diffusivity does not change with changing porosity for the expression $f_m = \phi * 0.0265$ (Fig. A3).

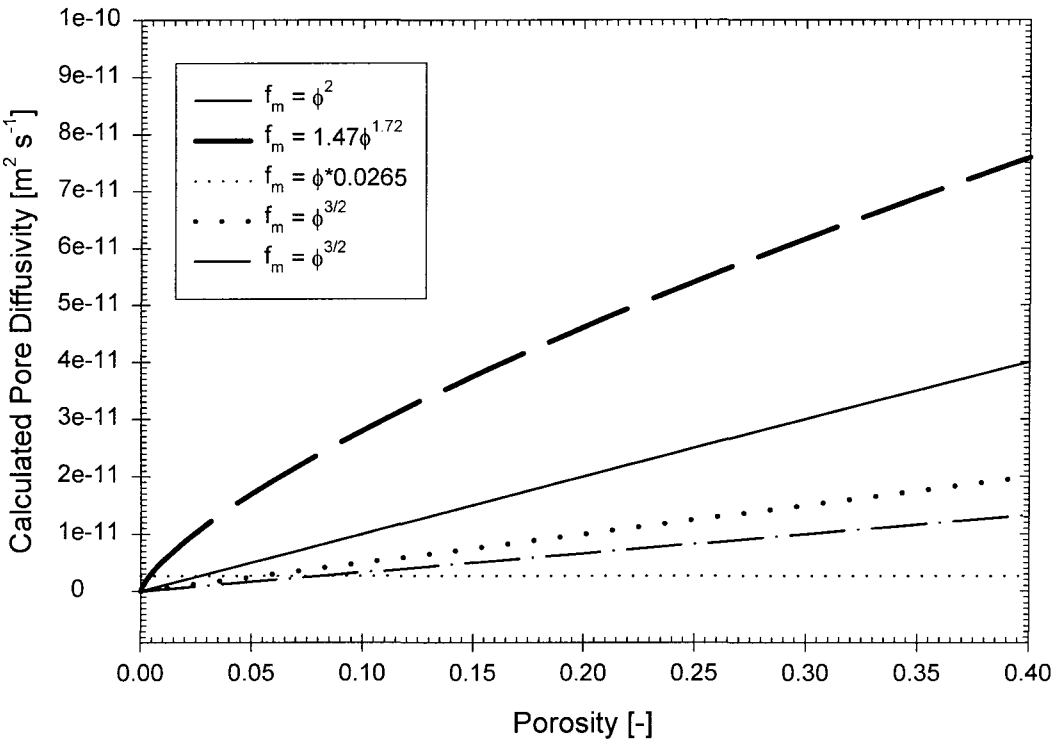

Figure A3. Pore diffusivities predicted for an aqueous diffusivity of $1.0x10^{-10}$ m^2 s^{-1} from the different relations between formation factor and porosity. Note that the expression $f_m = \phi*0.0265$ yields constant pore diffusivities for all porosities, while the expression $f_m = \phi^2$ gives a linear relation between porosity and pore diffusivity. The expression $f_m = 1.47\phi^{1.72}$ (thick dashed line) yields the highest pore diffusivities.

Concluding Remarks

An empirical expression for the relation between the formation factor and porosity at low porosities was derived. This allows the estimation of the diffusivity for a single, non-reactive solute from porosity values only. In comparison to other known relations (Van Barkel and Heertjes, 1974), this new non-linear expression appears to yield slightly better results for very low-porosity rocks, since the common relations are derived for high-porosity rocks. It can therefore be applied to reactive transport modeling in crystalline rocks where porosities change only slightly during hydrothermal alteration or metamorphism.

References

Cussler, E.L., 1996, Diffusion: Mass transfer in fluid Systems. Cambridge University Press, 525 pages.

Geiger, S., 2000, Reactive transport modeling in discrete fractures: Applications to the formation of sericitic hydrothermal alteration at Butte, Montana. MS Thesis, Dept. of Geosciences, Oregon State University, 124 pages.

Lasaga, A.C. and Rye, D.M., 1993, Fluid flow and chemical reaction kinetics in metamorphic systems. American Journal of Science, v. 293, 2169-2175.

Lichtner, P.C., 1996, Continuum formulation of multicomponent-multiphase reactive transport. In: Lichtner, P.C., Steefel, C.I., and Oelkers, E.H. (eds.), Reactive Transport in Porous Media. Reviews in Mineralogy, v. 34, 1-81.

Oelkers, E.H., 1996, Physical and chemical properties of rocks and fluids for chemical mass transport calculations. In: Lichtner, P. C., Steefel, C. I., and Oelkers, E. H. (eds.), Reactive Transport in Porous Media. Reviews in Mineralogy, v. 34, 131-191.

Ohlsson, Y. and Neretnieks, I., 1995, Literature survey of matrix diffusion theory and of experiments and data including natural analogues. Swedish Nuclear Fuel and Waste Management Corporation, SKB Technical Report 95-12, Sweden, 89 pages.

Skagius, K. and Neretnieks, I., 1986, Porosities and diffusivities of some nonsorbing species in crystalline rocks. Water Resources Research, v. 22, 389-398.

Steefel, C.I. and MacQuarrie, K.T.B., 1996, Approaches to modeling of reactive transport in porous media. In: Lichtner, P. C., Steefel, C. I., and Oelkers, E. H. (eds.), Reactive Transport in Porous Media. Reviews in Mineralogy, v. 34, 83-129.

Van Barkel, J. and Heertjes, P.M., 1974, Analysis of diffusion in macroporous media in terms of a porosity, a tortuosity and a constrictivity factor. International Journal of Heat Mass Transfer, v 17, 1082-1103.